Theory of the Earth

Don L. Anderson

Chapter 6. Elasticity and Solid-state Geophysics

Boston: Blackwell Scientific Publications, c1989

Recommended citation:

Anderson, Don L. Theory of the Earth. Boston: Blackwell Scientific Publications, 1989. http://resolver.caltech.edu/CaltechBOOK:1989.001

A scanned image of the entire book may be found at the following persistent URL:

http://resolver.caltech.edu/CaltechBook:1989.001

Abstract:

The seismic properties of a material depend on composition, crystal structure, temperature, pressure and in some cases defect concentrations. Most of the Earth is made up of crystals. The elastic properties of crystals depend on orientation and frequency. Thus, the interpretation of seismic data, or the extrapolation of laboratory data, requires knowledge of crystal or mineral physics, elasticity and thermodynamics. The physics of fluids is involved in the study of magmas and the outer core. In the previous chapter we concentrated on density and the bulk modulus. In the present chapter we delve into the shear modulus and the seismic velocities. The following chapter deals with transport and nonelastic properties. Later chapters on seismic wave attenuation, anisotropy and mantle mineralogy build on this foundation.

6

Elasticity and Solid-state Geophysics

Mark well the various kinds of minerals, note their properties and ***their*** *mode of origin.*

—PETRUS SEVERINUS *(1571)*

The seismic properties of a material depend on composition, crystal structure, temperature, pressure and in some cases defect concentrations. Most of the Earth is made up of crystals. The elastic properties of crystals depend on orientation and frequency. Thus, the interpretation of seismic data, or the extrapolation of laboratory data, requires knowledge of crystal or mineral physics, elasticity and thermodynamics. The physics of fluids is involved in the study of magmas and the outer core. In the previous chapter we concentrated on density and the bulk modulus. In the present chapter we delve into the shear modulus and the seismic velocities. The following chapter deals with transport and nonelastic properties. Later chapters on seismic wave attenuation, anisotropy and mantle mineralogy build on this foundation.

ELASTIC CONSTANTS OF ISOTROPIC SOLIDS

The elastic behavior of an isotropic solid is completely characterized by the density p and two elastic constants. These are usually the bulk modulus K and the rigidity G (or μ) or the two Lam6 parameters (which we will not use), λ and μ (= G). Young's modulus E and Poisson's ratio σ are also commonly used. There are, correspondingly, two types of elastic waves; the compressional, or primary (P), and the shear, or secondary (S), having velocities derivable from

$$\rho V_p^2 = K + 4G/3$$

$$\rho V_s^2 = G$$

The interrelations between the elastic constants and wave velocities are given in Table 6-1.

Only well-annealed glasses and similar noncrystalline materials are strictly isotropic. Crystalline material with random orientations of grains can approach isotropy, but rocks are generally anisotropic.

Laboratory measurements of mineral elastic properties, and their temperature and pressure derivatives, are an essential complement to seismic data. The elastic wave velocities are now known for hundreds of crystals. Although many of these are not directly relevant to measured seismic velocities, they are invaluable for developing rules that can be applied to the prediction of properties of unmeasured phases. Elastic properties depend on both crystal structure and composition, and the understanding of these effects, including the role of temperature and pressure, is a responsibility of a discipline called mineral physics or solid-state geophysics. Most measurements are made under conditions far from the pressure and temperature conditions in the deep crust or mantle. The measurements themselves, therefore, are just the first step in any program to predict or interpret seismic velocities.

Some information is now available on the elastic properties of all major rock-forming minerals in the mantle. On the other hand, there are insufficient data on any mineral to make assumption-free comparisons with seismic data below some 100 km depth. This is why it is essential to have a good theoretical understanding of the effects of temperature, composition and pressure on the elastic and thermal properties of minerals so that laboratory measurements can be extrapolated to mantle conditions. Laboratory results are generally given in terms of a linear dependence of the elastic moduli on temperature and pressure. The actual variation

TABLE 6-1
Connecting Identities for Elastic Constants of Isotropic Bodies

K	$G = \mu$	λ	σ
$\lambda+2\mu/3$	$3(K-\lambda)/2$	$K-2\mu/3$	$\dfrac{\lambda}{3(\lambda+\mu)}$
$\mu\dfrac{2(1+\sigma)}{3(1-2\sigma)}$	$\lambda\dfrac{1-2\sigma}{2\sigma}$	$\mu\dfrac{2\sigma}{1-2\sigma}$	$\dfrac{\lambda}{3K-\lambda}$
$\lambda\dfrac{1+\sigma}{3\sigma}$	$3K\dfrac{1-2\sigma}{2+2\sigma}$	$3K\dfrac{\sigma}{1+\sigma}$	$\dfrac{3K-2\mu}{2(3K+\mu)}$
$\rho(V_p^2-4V_s^2/3)$	ρV_s^2	$\rho(V_p^2-2V_s^2)$	—
—	—	—	$\dfrac{1}{2}\dfrac{(V_p/V_s)^2-2}{(V_p/V_s)^2-1}$

λ, μ = Lamé constants
G = Rigidity or shear modulus = $\rho V_s^2 = \mu$
K = Bulk modulus
σ = Poisson's ratio
E = Young's modulus
p = density
V_p, V_s = compressional and shear velocities

$$\rho V_p^2 = \lambda+2\mu = 3K-2\lambda = K+4\mu/3 = \mu\frac{4\mu-E}{3\mu-E}$$
$$= 3K\frac{3K+E}{9K-E} = \lambda\frac{1-\sigma}{\sigma} = \mu\frac{2-2\sigma}{1-2\sigma} = 3K\frac{1-\sigma}{1+\sigma}$$

of the moduli with temperature and pressure is more complex. Since the higher order and cross terms are not known in the Taylor series expansion of the moduli in terms of temperature and pressure and it is not reasonable to assume that all derivatives are independent of temperature and pressure, it is necessary to use physically based equations of state. Unfortunately, many discussions of upper-mantle mineralogy ignore the most elementary considerations of solid-state and atomic physics. For example, the functional form of $\alpha(T)$, the coefficient of thermal expansion, is closely related to the specific heat function, and the necessary theory was developed long ago by Debye, Griineisen and Einstein. Yet a is often assumed to be independent of temperature, or linearly dependent on temperature. Likewise, interatomic potential theory shows that dK/dP must decrease with compression, yet the moduli are often assumed to increase linearly with pressure throughout the upper mantle. There are also various thermodynamic relationships that must be satisfied by any self-consistent equation of state, and certain inequalities regarding the strain dependence of anharmonic properties.

Processes within the Earth are not expected to give random orientations of the constituent anisotropic minerals. On the other hand the full elastic tensor is difficult to determine from seismic data. Seismic data usually provide some sort of average of the velocities in a given region and, in some cases, estimates of the anisotropy.

The best quality laboratory data is obtained from high-quality single crystals. The full elastic tensor can be obtained in these cases, and methods are available for computing average properties from these data. A large amount of data exists on average properties from shock-wave and static-compression experiments, and it is useful to compare these results, sometimes on polycrystals or aggregates, with the single-crystal data.

It is simpler to tabulate and discuss average properties, as I do in this section. It should be kept in mind, however, that mantle minerals are anisotropic and they tend to be readily oriented by mantle processes. Certain seismic observations in subducting slabs, for example, are best interpreted in terms of oriented crystals and a resulting seismic anisotropy. If all seismic observations are interpreted in terms of isotropy, it is possible to arrive at erroneous conclusions. The debates about the thickness of the lithosphere, the deep structure of continents, the depth of slab penetration, and the scale of mantle convection are, to some extent, debates about the anisotropy of the mantle and the interpretation of seismic data. Although it is important to understand the effects of temperature and pressure on physical properties, it is also important to realize that changes in crystal structure (solid-solid phase changes) and orientation have large effects on the seismic velocities.

Table 6-2 is a compilation of the elastic properties, measured or estimated, of most of the important mantle

TABLE 6-2
Elastic Properties of Mantle Minerals (Duffy and Anderson, 1988)

Formula (structure)	Density[1] (g/cm^3)	K_S (GPa)	G (GPa)	K_s'	G'	$-\dot{K}_S$ (GPa/K)	$-\dot{G}$ (GPa/K)
$(Mg,Fe)_2SiO_4$ (olivine)	$3.222(2) + 1.182x_{Fe}$	129(2)[2]	$82(1) - 31(1)x_{Fe}^2$	5.1(3)[3]	1.8(1)[3]	0.016(1)[4]	0.013(1)[5]
$(Mg,Fe)_2SiO_4$ (β-spinel)	$3.472(5) + 1.24(9)x_{Fe}$	174(1)[6]	$114(1) - 41x_{Fe}^7$	4.9	1.8	0.018	0.014
$(Mg,Fe)_2SiO_4$ (y-spinel)	$3.548(1) + 1.30x_{Fe}$	184(1)[8]	$119(1) - 41x_{Fe}^8$	4.8	1.8	0.017	0.014
$(Mg,Fe)SiO_3$ (orthopyroxene)	$3.204(5) + 0.799(5)x_{Fe}$	104(4)[9]	$77(1) - 24(1)x_{Fe}^9$	5.0	2.0	0.012	0.011
$CaMgSi_2O_6$ (clinopyroxene)	3.277(5)[10]	113(1)[11]	67(2)[11]	4.5(1.8)[12]	1.7	0.013	0.010
$NaAlSi_2O_6$ (clinopyroxene)	3.32(2)[10]	143(2)[13]	84(2)[13]	4.5	1.7	0.016	0.013
(Mg,Fe)O (magnesiowustite)	$3.583(1) + 2.28(1)x_{Fe}$	$163(1) - 8(5)x_{Fe}^{14}$	$131(1) - 77(5)x_{Fe}^{14}$	4.2(3)[11]	2.5(1)[11]	0.016(3)[11]	0.024(4)[11]
Al_2O_3 (corundum)	3.988(2)[10]	251(3)[11]	162(2)[11]	4.3(1)[11]	1.8(1)[11]	0.014(3)[11]	0.019(1)[11]
SiO_2 (stishovite)	4.289(3)	316(4)[11]	220(3)[11]	4.0	1.8	0.027	0.018
$(Mg,Fe)_3Al_2Si_3O_{12}$ (garnet)	$3.562(2) + 0.758(3)x_{Fe}$	$175(1) + 1(1)x_{Fe}^{11}$	$90(1) + 8(1)x_{Fe}^{11}$	4.9(5)[11]	1.4(1)[11]	0.021(2)[11]	0.010(1)[11]
$Ca_3(Al,Fe)_2Si_3O_{12}$ (garnet)	$3.595(2) + 0.265(1)x_{Fe}^{10}$	$169(2) - 11(2)x_{Fe}^{15}$	$104(1) - 14(1)x_{Fe}^{15}$	4.9	1.6	0.016[16]	0.015[16]
$(Mg,Fe)SiO_3$ (ilmenite)	$3.810(4) + 1.10(5)x_{Fe}$	212(4)[17]	$132(9) - 41x_{Fe}^{17}$	4.3	1.7	0.017	0.017
$(Mg,Fe)SiO_3$ (perovskite)	$4.104(7) + 1.07(6)x_{Fe}$	266(6)[18]	153	3.9(4)[18]	2.0	0.031	0.028
$CaSiO_3$ (perovskite)	4.13(11)[19]	227	125	3.9	1.9	0.027	0.023
$(Mg,Fe)_4Si_4O_{12}$ (majorite)	$3.518(3) + 0.973(7)x_{Fe}$	$175 + 1x_{Fe}^{20}$	$90 + 8x_{Fe}^{20}$	4.9	1.4	0.021	0.010
$Ca_2Mg_2Si_4O_{12}$ (majorite)	3.53[21]	165	104	4.9	1.6	0.016	0.015
$Na_2Al_2Si_4O_{12}$ (majorite)	4.00[21]	200	127	4.9	1.6	0.016	0.015

(1) All densities from Jeanloz and Thompson (1983) except where indicated; x_{Fe} is molar fraction of Fe endmember.
(2) Graham and others (1982), Schwab and Graham (1983), Suzuki and others (1983), Sumino and Anderson (1984), and Yeganeh-Haeri and Vaughan (1984).
(3) Schwab and Graham (1983), Sumino and Anderson (1984).
(4) Suzuki and others (1983), Sumino and Anderson (1984); $\dot{K} = \partial K/\partial T$.
(5) Schwab and Graham (1983), Suzuki and others (1983), Sumino and Anderson (1984); $\dot{G} = \partial G/\partial T$.
(6) Sawamoto and others (1984).
(7) Sawamoto and others (1984). The effect of Fe on the modulus is from Weidner and others (1984).
(8) Weidner and others (1984).
(9) Sumino and Anderson (1984), Bass and Weidner (1984), Duffy and Vaughan (1986).
(10) Robie and others (1966).
(11) Sumino and Anderson (1984).
(12) Levine and Prewitt (1981).
(13) Kandelin and Weidner (1984).
(14) Sumino and Anderson (1984).
(15) Halleck (1973), Bass (1986).
(16) Isaak and Anderson (1987).
(17) Weidner and Ito (1985).
(18) Knittle and Jeanloz (1987).
(19) Bass (1984).
(20) Inferred from Weidner and others (1987).
(21) Estimated by Bass and Anderson (1984).

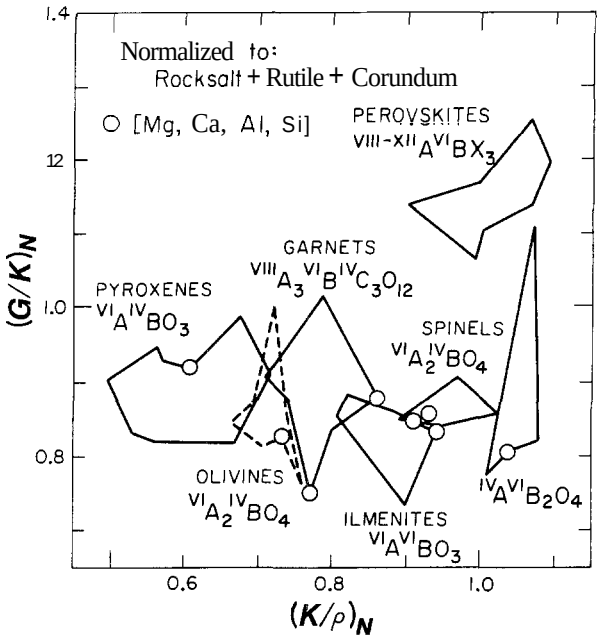

FIGURE 6-1
GIK versus *Klp*, normalized to values of constituent oxides or fluorides. Note the relatively small range of *(GIK)*, for Mg, Ca, Al and Si oxides. There is also little change of GIK associated with phase changes. This plot suggests a method for estimating rigidities for unmeasured phases.

minerals. Figure 6-1 relates rigidity to bulk modulus and density of major minerals.

TEMPERATURE AND PRESSURE DERIVATIVES OF ELASTIC MODULI

The pressure derivatives of the adiabatic bulk modulus, $K'_S = dK_S/dP$, for halides and oxides generally fall in the range 4.0 to 5.5. Rutiles are generally somewhat higher, 5 to 7. Oxides and silicates having ions most pertinent to major mantle minerals have a much smaller range, usually between 4.3 and 5.4. MgO has an unusually low K'_S, 3.85. The density derivative of the bulk modulus,

$$(\partial \ln K_S/\partial \ln \rho)_T = (K_T/K_S)K'_S$$

for mantle oxides and silicates that have been measured usually fall between 4.3 and 5.4 with MgO, 3.8, again being low.

The rigidity, G, has a much weaker volume or density dependence. The parameter

$$(\partial \ln G/\partial \ln \rho)_T = (K_T/G)G'$$

generally falls between about 2.5 and 2.7. For the above subset of minerals

$$(\partial \ln K_S/\partial \ln G)_T = K_S/G$$

is a very good approximation. More generally,

$$G'/K'_S = (G/K_S)^a$$

where $a \approx 2$ to 3 for most minerals (see Figure 6-2). These relations are useful since we know K' and KIG for many minerals for which G' is unknown.

The intrinsic temperature derivatives

$$(\partial \ln M/\alpha \partial T)_v$$

are generally negative for K_T (-4 to -1) and always negative for G (-2 to -4). The range for K_S is $+1.5$ to -2. The dimensionless intrinsic temperature derivatives are generally close to zero for K_S and about -3.4 ± 2 for G. These ranges are for most oxides, halides and silicates. The inequality

$$\left(\frac{\partial \ln K_S}{\alpha \partial T}\right)_v > \left(\frac{\partial \ln G}{\alpha \partial T}\right)_v$$

holds except for some perovskites. The magnitude of the temperature derivatives, at constant volume, indicates the intrinsic effect of temperature.

The pressure derivative of the rigidity is low for $MgAl_2O_4$-spinel. This is probably because of the low (tetrahedral) coordination of Mg. In most mantle minerals Mg exhibits 6- to 12-fold coordination, a topic considered in detail in Chapter 16.

The normalized temperature and pressure derivatives expose the intrinsic effects of temperature and show that these are generally greater for the rigidity than the bulk modulus. The normalized derivatives show a strong dependence on the constituent ions but only a weak dependence on crystal structure.

The relative changes in moduli with respect to temperature, $\partial \ln K_S/\partial T$ and $\partial \ln G/\partial T$, are of the order of

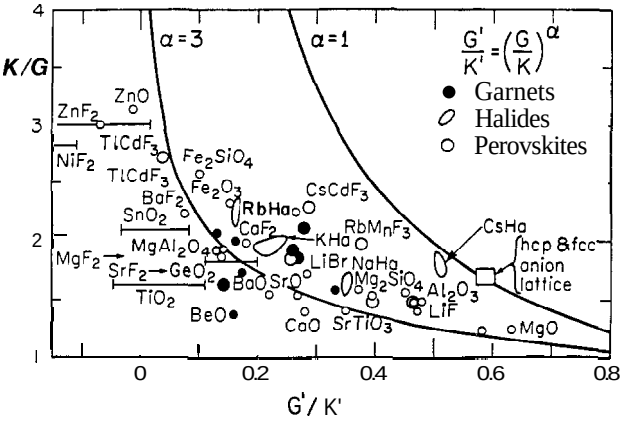

FIGURE 6-2
Correlation between *G'IK'* and *KIG* for crystals. The clustering of the alkali halides suggests cation control on these properties.

TABLE 6-3
Estimated Elastic Properties from High-pressure Experiments

Formula	Structure	ρ_o (g/cm^3)	K_o (GPa)	K_o'	γ	Source
CaO	B2	3.76	115.0	4.9	1.8	1
	B1	3.35	112	4.8	1.5	7
FeO	B2	6.05	195.0	3.4	1.8	1
	B1	5.86	185	3.2	1.6	7
MgO	B1	3.583	163.0	4.2	1.5	1
Al_2O_3	co	3.99	253.2	3.9	1.5	6
SiO_2	st	4.29	316.0	4.0	1.5	1
$CaSiO_3$	pv	4.17	220.0	4.0	1.2	1
			263.0	4.13		3
$FeSiO_3$	pv	5.23	250.0	4.0	1.2	1
$MgSiO_3$	pv	4.10	260.0	4.0	1.2	1
			266.0	3.9	1.8	4
$CaMgSi_2O_6$	m.ox.	4.00	207.5	4.2	1.6	1
$CaMgSi_2O_6$	pv	4.12	237.7	4.0	1.2	1
$CaFeSi_2O_6$	m.ox.	4.53	214.2	4.0	1.6	1
$CaFeSi_2O_6$	pv	4.65	233.6	4.0	1.6	1
Fe_2SiO_4	ol	—	119	7	—	5
$CaMgSi_2O_6$	cpx	—	114.0	4.5	—	2
$FeSiO_4$	sp.	—	192.0	6.3	—	2
$Mg_3Al_2Si_3O_{12}$	gt	—	175.0	4.5	—	2
TiO_2	ru	—	209.0	7.3		2

(1) Svendsen and Ahrens (1983).
(2) Bass and others (1981).
(3) Wolf and Bukowinski (1986).
(4) Knittle and Jeanloz (1986).
(5) Yagi and others (1975).
(6) Ahrens and others (1969).
(7) Jeanloz and Ahrens (1980).

-1.5 (± 0.6) $\times$ 10^{-4}/°C. These are analogous to the coefficient of thermal expansion, $a = d \ln \rho/\partial T$, but are typically five to eight times larger. These normalized moduli derivatives increase with temperature and approach a constant value at high temperature. The fully normalized derivatives,

$$(\partial \ln M/\partial \ln \rho)_P = (\partial \ln M/\alpha \partial T)_P$$

are typically 6.2 ± 0.2 for oxides and silicates. The above values are illustrative. Tables 6-3 and 6-4 give more complete compilations. The fully normalized derivatives are similar to Grüneisen parameters and might be expected to be relatively constant from material to material and as a function of temperature, at least at high temperature.

INTRINSIC AND EXTRINSIC TEMPERATURE EFFECTS

The effects of temperature on the properties of the mantle must be known for various geophysical calculations. Because the lower mantle is under simultaneous high pressure and high temperature, it is not clear that the simplifications that can be made in the classical high-temperature limit are necessarily valid. For example, the coefficient of thermal expansion, which controls many of the anharmonic properties, increases with temperature but decreases with pressure. At high temperature, the elastic properties depend mainly on the volume through the thermal expansion. At high pressure, on the other hand, the intrinsic effects of temperature may become relatively more important.

The temperature derivatives of the elastic moduli can be decomposed into extrinsic and intrinsic components:

$$(\partial \ln K_S/\partial \ln \rho)_P = (\partial \ln K_S/\partial \ln \rho)_T - \alpha^{-1}(\partial \ln K_S/\partial T)_V$$

for the adiabatic bulk modulus, K_S, and a similar expression for the rigidity, G. Extrinsic and intrinsic effects are sometimes called "volumetric" or "quasi-harmonic" and "anharmonic," respectively.

The intrinsic contribution is

$$(d \ln M/\partial T)_V = \alpha[(\partial \ln M/\partial \ln \rho)_T - (\partial \ln M/\partial \ln \rho)_P] \quad (1)$$

where M is K, or G. There would be no intrinsic or an-

TABLE 6-4
Pressure Derivatives of Moduli of Cubic Crystals

Formula	C_{11}'	$(C_{11}-C_{12})'/2$	C_{44}'	K_S'	K	G
Rocksalt structures						
LiF	9.97	2.73	1.38	5.14	.70	.49
MgO	8.70	3.64	1.09	3.85	1.63	1.31
NaF	11.56	1.99	0.21	5.18	.48	.31
CaO	10.53	3.4	0.6	6.0	1.14	.81
KF	12.26	5.25	−0.43	5.26	.31	.17
SrO	11.33	4.0	--0.2	6.0	0.88	.59
RbF	12.14	4.93	−0.7	5.57	.27	.13
Perovskite structures						
$KMgF_3$	8.93	2.94	1.31	5.01	.75	.47
$RbMnF_3$	10.19	3.95	0.75	4.92	.68	.34
$SrTiO_3$	10.21	3.35	1.24	5.74	1.74	1.17

Davies (1976), Jones (1976, 1979).
K, G are moduli in Mbar.

harmonic effect if $a = 0$ or if $(\partial \ln M/\partial \ln p)_T = (\partial \ln M/\partial \ln p)_S$, that is, $M(V,T) = M(V)$.

It is often assumed that αK_T is independent of pressure. This yields $\delta_T = K_T'$. When this holds there is no intrinsic temperature dependence of K_T, which is then a function of volume alone. Seismic data and most laboratory data aefer to adiabatic conditions, and we will henceforth deal only with the adiabatic constants. Note that $\delta_T = K_T'$ does not imply $\delta_S = K_S'$.

The various terms in equation 1 require measurements as a function of both temperature and pressure. These are tabulated in Table 6-5 for a variety of oxides and silicates. Generally,

$$|[\partial \ln G/\partial T]_V| > |[\partial \ln K_S/\partial T]_V|$$

The intrinsic temperature effect on rigidity is greater than on the bulk modulus; **G** is a weaker function of volume at constant T than at constant P; and G is a weaker function of volume, at constant *T,* than is the bulk modulus.

The extrinsic terms are functions of pressure through the moduli and their pressure derivatives. This pressure dependence can be exposed by writing the extrinsic or quasi-harmonic terms as:

$$\alpha(K_T/K_S)(\partial K_S/\partial P)_T = -\hat{K}_{ex}$$

$$\alpha(K_T/G)(\partial G/\partial P)_T = -\hat{G}_{ex}$$

Both K_S' and **G**' decrease by about 30 percent from $P = 0$ to the base of the lower mantle (Dziewonski and Anderson, 1981). The coefficient of thermal expansion, at constant temperature, decreases by about 80 percent (Birch, 1968). The term K_T/G increases by about 30 percent. The net effect is an appreciable decrease for $\hat{K}_{ex}$ and a slightly smaller decrease for $\hat{G}_{ex}$. Using lower-mantle parameters from PREM, $a = 4 \times 10^{-5}$/K and the extrapolations of Butler and Anderson (1978), we obtain -0.2×10^{-3}/deg for the high-temperature, zero-pressure value of $\hat{K}_{ex}$, similar to values for perovskites (Jones, 1979). At the core-mantle boundary (CMB) this is reduced to -0.02×10^{-3}/deg, comparable in magnitude to laboratory measurements of intrinsic temperature derivatives. The calculated zero-pressure value for $\hat{G}_{ex}$ of the lower mantle is -0.1×10^{-3}/deg decreasing to -0.02×10^{-3}/deg at the CMB. These results show that the extrinsic effects of temperature on elastic moduli become very small at lower-mantle conditions. The assumption that the adiabatic elastic moduli depend only on volume is likely to be a poor approximation. The intrinsic temperature derivatives also decrease with compression (Zharkov and Kalinin, 1971).

The inferred intrinsic temperature effect on the bulk modulus is generally small and can be either negative or positive (Table 6-5). The bulk modulus and its derivatives must be computed from differences of the directly measured moduli and therefore they have much larger errors than the shear moduli. The intrinsic temperature derivatives of the bulk modulus account for 25–40 percent of the total temperature effect for the rutiles and $SrTiO_3$-perovskite. For these structures an increase in temperature at constant volume decreases the bulk modulus. Other perovskites have positive values for $(\partial \ln K_S/\partial T)_V$ (Jones, 1979).

The intrinsic component of the temperature derivative of the rigidity is often larger than the extrinsic, or volume dependent, component and is invariably negative; an increase in temperature causes G to decrease due to the decrease in density, but a large part of this decrease would occur at constant volume. Increasing pressure decreases the total temperature effect because of the decrease of the extrinsic component and the coefficient of thermal expansion. The net effect is a reduction of the temperature derivatives, and a larger role for rigidity in controlling the temperature

variation of seismic velocities and Griineisen ratios in the lower mantle. This explains some recent data from seismic tomography. Note that $\alpha^{-1}\ (\partial \ln G/\partial T)_V$ exhibits little variation for the materials in Table 6-5. It is generally larger, in absolute value, than $\alpha^{-1}\ (\partial \ln K_S/\partial T)_V$ and of opposite sign. High temperature, at constant volume, makes most solids harder to compress adiabatically but easier to shear.

The total effects of temperature on the bulk modulus and on the rigidity, $(\partial \ln M/\partial \ln p)$,, are comparable under laboratory conditions (Table 6-5). Therefore the compressional and shear velocities have similar temperature dependencies. On the other hand, the thermal effect on bulk modulus is largely extrinsic, that is, it depends mainly on the change in volume due to thermal expansion. The shear modulus is affected both by the volume change and a purely thermal effect at constant volume.

Although the data in Table 6-5 are not in the classical high-temperature regime $(T/\theta \gg 1)$, it is still possible to separate the temperature derivatives into volume-dependent and volume-independentparts. Measurementsmust be made at much higher temperatures in order to test the various assumptions involved in quasi-harmonic approximations. One of the main results I have shown here is that, in general, the relative roles of intrinsic and extrinsic contributions and the relative temperature variations in bulk and shear moduli will not mimic those found in the restricted range of temperature and pressure presently available in the laboratory. The Earth can be used as a natural laboratory to extend conventional laboratory results.

It is convenient to treat thermodynamic parameters, including elastic moduli, in terms of volume-dependent and temperature-dependent parts, as in the Mie-Griineisen equation of state. This is facilitated by the introduction of dimensionless anharmonic (DA) parameters. The Griineisen ratio γ is such a parameter. $\partial K/\partial P = K'$ and $\partial G/\partial P =$ G' are also dimensionless anharmonic parameters, but it is useful to replace pressure, and temperature, by volume. This is done by forming logarithmic derivatives with respect to volume or density, giving Dimensionless Logarithmic An-

TABLE 6-5
Extrinsic and Intrinsic Components of $(\partial \ln M/\partial \ln \rho)_P$

	Extrinsic		*Intrinsic*	
Substance	$\left(\frac{\partial \ln K_S}{\partial \ln \rho}\right)_P$	$\left(\frac{\partial \ln K_S}{\partial \ln \rho}\right)_T$	$\frac{1}{\alpha}\left(\frac{\partial \ln K_S}{\partial T}\right)_V$	$\left(\frac{\partial \ln K_S}{\partial T}\right)_V$ (10^{-5}/deg)
MgO	3.0	3.8	0.8	2.3
CaO	3.9	4.8	0.9	2.6
SrO	4.7	5.1	0.4	1.6
TiO_2	10.5	6.8	−3.7	−8.7
GeO_2	10.2	6.1	−4.1	−5.6
Al_2O_3	4.3	4.3	0.0	0.0
Mg_2SiO_4	4.7	5.4	0.7	0.03
$MgAl_2O_4$	4.0	4.2	0.2	0.4
Garnet	5.2	5.5	0.3	0.5
$SrTiO_3$	7.9	5.7	−2.2	−6.2
Substance	$\left(\frac{\partial \ln G}{\partial \ln \rho}\right)_P$	$\left(\frac{\partial \ln G}{\partial \ln \rho}\right)_T$	$\frac{1}{\alpha}\left(\frac{\partial \ln G}{\partial T}\right)_V$	$\left(\frac{\partial \ln G}{\partial T}\right)_V$ (10^{-5}/deg)
MgO	5.8	3.0	−2.8	−8.6
CaO	6.3	2.4	−3.9	−11.2
SrO	4.9	2.2	−2.7	−11.3
TiO_2	8.4	1.2	−7.2	−16.9
GeO_2	5.8	2.1	−3.7	−5.1
Al_2O_3	7.5	2.6	−4.9	−16.5
Mg_2SiO_4	6.5	2.8	−3.7	−9.2
$MgAl_2O_4$	5.9	1.3	−4.6	−7.4
Garnet	5.4	2.6	−2.8	−6.1
$SrTiO_3$	7.9	3.1	−4.8	−13.4

Sumino and Anderson (1984).

TABLE 6-6
Normalized Pressure and Temperature Derivatives

Substance	$\left(\frac{\partial \ln K_S}{\partial \ln \rho}\right)_T$	$\left(\frac{\partial \ln G}{\partial \ln \rho}\right)_T$	$\left(\frac{\partial \ln K_S}{\partial \ln G}\right)_T$	$\frac{K_S}{G}$	$\left(\frac{\partial \ln K_S}{\partial \ln \rho}\right)_P$	$\left(\frac{\partial \ln G}{\partial \ln \rho}\right)_P$	$\left(\frac{\partial \ln K_S}{\alpha \partial T}\right)_V$	$\left(\frac{\partial \ln G}{\alpha \partial T}\right)_V$
MgO	3.80	3.01	1.26	1.24	3.04	5.81	0.76	−2.81
Al_2O_3	4.34	2.71	1.61	1.54	4.31	7.45	0.03	−4.74
Olivine	5.09	2.90	1.75	1.64	4.89	6.67	0.2	−3.76
Garnet	4.71	2.70	1.74	1.85	6.84	4.89	−2.1	−2.19
$MgAl_2O_4$	4.85	0.92	5.26	1.82	3.84	4.19	1.01	−3.26
$SrTiO_3$	5.67	3.92	1.45	1.49	8.77	8.70	−3.1	−4.78

harmonic (DLA) parameters. They are formed as follows:

$$(\partial \ln M/\partial \ln \rho)_T = \frac{K_T}{M}\left(\frac{\partial M}{\partial P}\right)_T = \{M\}_T$$

$$(\partial \ln M/\partial \ln \rho)_P = (\alpha M)^{-1}\left(\frac{\partial M}{\partial T}\right)_P = \{M\}_P$$

$$(\partial \ln M/\alpha \partial T)_V = \{M\}_T - \{M\}_P = \{M\}_V$$

where we use braces $\{\}$ to denote DLA parameters and the subscripts T, P, V and S denote isothermal, isobaric, isovolume and adiabatic conditions, respectively. The $\{\}_V$ terms are known as intrinsic derivatives, giving the effect of temperature or pressure at constant volume. Derivatives for common mantle minerals are listed in Table 6-6. Elastic, thermal and anharmonic parameters are relatively independent of temperature at constant volume, particularly at high temperature. This simplifies temperature corrections for the elastic moduli. I use density rather than volume in order to make most of the parameters positive. By high temperature I mean $T > \theta$ where 8 is the Debye or Einstein temperature. The dimensionless Griineisen parameter γ is generally relatively constant over a broader temperature range than other thermal parameters such as a and C_P.

The DLA parameters relate the variation of the moduli to volume, or density, rather than to temperature and pressure. This is useful since the variations of density with temperature, pressure, composition and phase are fairly well understood. Furthermore, anharmonic properties tend to be independent of temperature and pressure at constant volume. The anharmonic parameter known as the thermal Grüneisen parameter γ is relatively constant from material to material as well as relatively independent of temperature.

SEISMIC CONSTRAINTS ON THERMODYNAMICS OF THE LOWER MANTLE

For most solids at normal conditions, the effect of temperature on the elastic properties is controlled mainly by the variation of volume. Volume-dependent extrinsic effects dominate at low pressure and high temperature. Under these conditions one expects that the relative changes in shear velocity, due to lateral temperature gradients in the mantle, should be similar to changes in compressional velocity. **However, at high pressure, this contribution is suppressed,** particularly for the bulk modulus, and variations of seismic velocities are due primarily to changes in the rigidity. Seismic data for the lower mantle can be used to estimate the Griineisen parameters and related parameters such as the temperature and pressure derivatives of the elastic moduli and thermal expansion.

In an earlier section I showed how the bulk modulus K depended on volume through changes in temperature and pressure and how these changes, $(\partial \ln Kld \ln V)$, and $(\partial \ln K/\partial \ln V)_P$, were related to the Griineisen parameters and the coefficient of thermal expansion a. The extrinsic, or volume-dependent, effects were shown to be greater than the intrinsic temperature effects. These considerations are now extended to the shear properties so that individual seismic wave velocities can be treated. Intrinsic effects are more important for the rigidity than for the bulk modulus. Recent geophysical results on the radial and lateral variations of velocity and density provide new constraints on high pressure–high temperature equations of state. Many of the thermodynamic properties of the lower mantle, required for equation-of-state modeling, can be determined directly from the seismic data. The effect of pressure on the coefficient of thermal expansion, the Griineisen parameters, the lattice conductivity and the temperature derivatives of seismic wave velocities should be taken into account in the interpretation of seismic data and in convection and geoid calculations.

The lateral variation of seismic velocity is very large in the upper 200 km of the mantle but decreases rapidly below this depth. Velocity itself generally increases with depth below about 200 km. This suggests that temperature variations are more important in the shallow mantle than at greater depth. Most of the mantle is above the Debye temperature and therefore thermodynamic properties may approach their classical high-temperature limits. On the other hand, the theoretical properties of solids at simultaneous

high pressure and temperature are seldom treated, and there are few precise data on variations of properties with temperature at these extreme conditions.

The effects of temperature on the bulk modulus and rigidity, that is, $(\partial \ln K/\partial T)_P$ and $(\partial \ln G/\partial T)_P$, are comparable for most minerals under normal conditions. This means that the relative variation of compressional and shear velocity with temperature should be similar. Doyle and Hales (1967), however, found that shear wave travel time anomalies, At_s, are about four times the compressional wave anomalies, At_p. This requires that lateral variations in rigidity are greater than lateral variations in compressibility or bulk modulus. The interpretation was that the anomalies are dominated by a partially molten region in the upper mantle, as partial melting affects the rigidity more than the bulk modulus. If only the rigidity changes, then

$$At_s = 3.9\ At_p$$

and

$$\mathrm{d} \ln V_s = 2.25\ \mathrm{d} \ln V_p$$

for Poisson's ratio $\sigma = 114$, or, equivalently, $(V_p/V_s)^2 = 3$ and $K = (5/3)G$. Yet a similar result has been found for the lower mantle, where the partial-melt explanation is less likely. We therefore seek a more general explanation for the apparently low lateral variation in K_s, the adiabatic bulk modulus.

The following parameters can be determined from seismology:

1. $(\partial K_S/\partial P)_S$ and $(\partial G/\partial P)_S$ from the radial variation of seismic velocities, assuming an adiabatic gradient. $(\partial K_S/\partial P)_T$ and $(\partial G/\partial P)_T$ are calculable from these.
2. $(\partial K_S/\partial T)_P$ and $(\partial G/\partial T)_P$ from the lateral changes in velocity, assuming these are due to temperature.

These derivatives are related to the Grüneisen parameters, y and 6, and the pressure derivative of the coefficient of thermal expansion, a. The derivatives of the rigidity, G, can also be cast into Griineisen-like parameters and used to test various assumptions in lattice dynamics, such as the assumption that longitudinal and transverse modes have the same volume dependence, or that lattice vibration frequencies depend only on volume.

We use the following relations and notation:

$$(\partial \ln K_T/\partial \ln \rho)_T = (\partial K_T/\partial P)_T = K_T' = \{K_T\}_T$$

$$(\partial \ln K_S/\partial \ln \rho)_T = (K_T/K_S)K_S' = \{K_S\}_T \quad (2)$$

$$(\partial \ln K_S/\partial \ln \rho)_P = -(\alpha K_S)^{-1}(\partial K_S/\partial T)_P = \delta_S = \{K_S\}_P \quad (3)$$

$$(\partial \ln G/\partial \ln \rho)_T = (K_T/G)(\partial G/\partial P)_T = (K_T/G)G' = G^* = \{G\}_T \quad (4)$$

$$(\partial \ln G/\partial \ln \rho)_P = -(\alpha G)^{-1}(\partial G/\partial T)_P = g = \{G\}_P \quad (5)$$

$$(\partial \ln K_T/\partial T)_P = (\partial \alpha/\partial \ln \rho), \quad (6)$$

$$\gamma = (1/2)K_S' - 1/6 + f(K,G,K',G') \quad (7)$$

$$-(\partial \ln \alpha/\partial \ln \rho)_T \approx \delta_S + \gamma = -\{\alpha\}_T \quad (8)$$

$$(\partial \ln K_T/\partial T)_V = \alpha[(\partial \ln K_T/\partial \ln \rho)_T - (\partial \ln K_T/\partial \ln \rho)_P] = \alpha(K_T' - \delta_T) \quad (9)$$

$$(\partial \ln G/\partial T)_V = \alpha[(\partial \ln G/\partial \ln \rho)_T - (\partial \ln G/\partial \ln \rho)_P] \quad (10)$$

$$K_S = K_T(1 + \alpha\gamma T) \quad (11)$$

$$\delta_T \approx \delta_S + \gamma \quad (12)$$

$$(\partial \ln K_S/\partial \ln \rho)_S = (\partial \ln K_S/\partial \ln p), + T\gamma(\partial \ln K_S/\partial T)_V = \{K_S\}_S \quad (13)$$

$$(\partial \ln G/\partial \ln \rho)_S = (\partial \ln G/\partial \ln p), + T\gamma(\partial \ln G/\partial T)_V = \{G\}_S \quad (14)$$

This notation stresses the volume, or density, dependence of the thermodynamic variables and is particularly useful in geophysical discussions as discussed earlier. The notation is: pressure, P, temperature, T, density, ρ, bulk modulus, K_S or K_T, rigidity, G, thermal expansion coefficient, a, and volume, V.

Values of most of the dimensionless logarithmic parameters are listed in Table 6-7 for many halides, oxides and minerals. Average values for chemical and structural classes are extracted in Table 6-8, and parameters for mineral phases of the lower mantle are presented in Table 6-9. Figures 6-3 to 6-5 show selected derivatives from Table 6-7 graphed against each other; Figure 6-6 relates some parameters to ionic radii and crystal structure.

The lateral variation of seismic velocities in the mantle can now be mapped with seismic tomographic techniques (Nakanishi and Anderson, *1982;* Clayton and Comer, *1983;* Dziewonski, *1984).* The correlation of lower-mantle velocities with the geoid has yielded estimates of $(\partial V_p/\partial \rho)_P = 3$ (kmls)/(g/cm^3) (Hager and others, *1985;* Richards, *1986).* This corresponds to $(\partial \ln V_p/\partial \ln \rho)_P = 1.2$ using lower mantle values from PREM. This is lower than laboratory values by 60 to 300 percent.

The variation of the seismic velocities can be written in terms of the moduli:

$$(\partial \ln V_s/\partial \ln p) = \tfrac{1}{2}[(\partial \ln G/\partial \ln p) - 1]$$

TABLE 6-7
Dimensionless Logarithmic Anharmonic Parameters

Substance	α $(10^{-6}/K)$	K_S *(kbar)*	G (kbar)	$\{K_S\}_T$	T	$\{K_T\}_P$	$\{K_S\}_P$	$\{G\}_P$	$\{K_T\}_V$	$\{K_S\}_V$	$\{G\}_V$	$\{K-G\}_V$	K_S/G	γ *thermal*	γ *BR*
LiF	98	723	485	4.90	3.97	4.69	2.42	6.35	0.5	2.5	−2.4	4.9	1.49	1.66	1.92
NaF	98	483	314	4.96	2.62	5.80	3.75	5.06	−0.6	1.2	−2.4	3.6	1.54	1.51	1.37
KF	99	318	164	4.81	1.97	5.05	3.18	6.17	0.0	1.6	−4.2	5.8	1.94	1.50	1.12
RbF	95	280	127	5.35	1.63	4.77	2.97	5.95	0.8	2.4	−4.3	6.7	2.20	1.43	1.05
LiCl	134	318	193	4.65	4.45	5.40	3.32	6.84	−0.4	1.3	−2.4	3.7	1.65	1.82	2.11
NaCl	118	252	148	5.10	3.00	5.45	3.74	5.07	−0.1	1.4	−2.1	3.4	1.71	1.51	1.55
KCl	105	181	93	5.10	2.01	7.48	5.67	5.54	−2.0	−0.6	−3.5	3.0	1.95	1.39	1.17
RbCl	119	163	78	5.09	1.79	5.81	4.11	5.30	−0.4	1.0	−3.5	4.5	2.10	1.44	1.09
AgCl	93	440	81	6.21	2.83	10.6	7.94	11.0	−3.8	−1.7	−8.2	6.5	5.44	2.08	1.77
NaBr	135	207	114	4.63	3.15	7.34	5.28	4.24	−2.2	−0.7	−1.1	0.4	1.81	1.72	1.59
KBr	116	150	79	5.12	2.01	5.64	3.94	4.68	−0.2	1.2	−2.7	3.8	1.90	1.45	1.16
RbBr	113	137	65	5.05	1.81	6.27	4.54	5.96	−0.9	0.5	−4.2	4.7	2.09	1.47	1.09
NaI	138	161	91	5.11	3.22	4.79	2.75	5.41	0.6	2.4	−2.2	4.5	1.76	1.74	1.65
KI	126	122	60	4.82	2.29	5.95	4.05	4.89	−0.8	0.8	−2.6	3.4	2.02	1.41	1.26
RbI	119	111	50	5.14	1.97	6.17	4.49	6.05	−0.7	0.6	−4.1	4.7	2.21	1.51	1.17
CsCl	140	182	101	5.20	4.75	6.28	3.82	6.01	−0.6	1.4	−1.3	2.6	1.80	2.04	2.30
TlCl	158	240	92	6.00	4.45	7.78	5.18	7.35	−1.0	0.8	−2.9	3.7	2.60	2.46	2.31
CsBr	138	156	88	4.97	4.53	6.33	3.86	5.90	−0.9	1.1	−1.4	2.5	1.76	1.98	2.18
TlBr	170	224	88	5.80	5.39	7.51	4.75	6.36	−0.8	1.1	−1.0	2.0	2.55	2.76	2.66
CsI	138	126	72	5.06	4.51	6.40	3.86	6.09	−0.9	1.2	−1.6	2.8	1.73	1.94	2.18
MgO	31	1628	1308	3.80	3.01	5.48	3.04	5.81	−1.6	0.8	−2.8	3.6	1.24	1.52	1.41
CaO	29	1125	810	4.78	2.42	5.45	3.92	6.29	−0.6	0.9	−3.9	4.7	1.39	1.27	1.25
SrO	42	912	587	5.07	2.25	6.99	4.68	4.98	−1.8	0.4	−2.7	3.1	1.55	1.74	1.22
BaO	38	720	367	5.42	1.95	9.46	7.34	7.88	−3.9	−1.9	−5.9	4.0	1.96	1.56	1.17
Al_2O_3	16	2512	1634	4.34	2.71	6.84	4.31	7.45	−2.5	0.0	−4.7	4.8	1.54	1.27	1.33
Ti_2O_3	17	2076	945	4.10	2.23	7.78	6.66	12.9	−3.6	−2.6	−11	8.2	2.20	1.13	1.15
	33	2066	910	4.44	1.63	5.70	3.68	3.34	−1.2	0.8	−1.7	2.5	2.27	1.99	0.95
TiO_2	24	2140	1120	6.83	1.09	12.7	10.5	8.37	−5.7	−3.7	−7.3	3.6	1.91	1.72	0.96
GeO_2	14	2589	1509	6.12	2.10	11.9	10.2	5.83	−5.7	−4.1	−3.7	−0.3	1.72	1.17	1.27
SnO_2	10	2123	1017	5.09	1.25	9.90	8.64	6.21	−4.8	−3.6	−5.0	1.4	2.09	0.88	0.85
MgF_2	38	1019	547	5.01	1.34	5.36	4.17	3.83	−0.3	0.8	−2.5	3.3	1.86	1.22	0.87
NiF_2	23	1207	459	4.98	−1.4	8.80	7.47	1.96	−3.8	−2.5	−3.4	0.9	2.63	0.88	−0.2
ZnF_2	29	1052	394	4.51	0.13	9.49	8.23	4.73	−4.9	−3.7	−4.6	0.9	2.67	0.97	0.39
CaF_2	61	845	427	4.55	2.26	5.85	3.86	4.75	−1.1	0.7	−2.5	3.2	1.98	1.83	1.21
SrF_2	47	714	350	4.67	1.66	6.02	4.75	4.94	−1.2	−0.1	−3.3	3.2	2.04	1.30	0.98
CdF_2	66	1054	330	5.77	4.05	8.36	6.04	7.11	−2.2	−0.3	−3.1	2.8	3.19	2.45	2.10
BaF_2	61	581	255	4.89	0.88	6.52	4.54	3.83	−1.4	0.3	−3.0	3.3	2.28	1.80	0.71
Opx	48	1035	747	9.26	3.18	7.26	5.43	3.34	2.2	3.8	−0.2	4.0	1.39	1.87	1.95
Olivine	25	1294	791	5.09	2.90	6.70	4.89	6.67	−1.6	0.2	−3.8	4.0	1.64	1.16	1.49
Olivine	27	1292	812	4.83	2.85	6.61	4.67	6.27	−1.7	0.2	−3.4	3.6	1.59	1.25	1.44
Olivine	25	1286	811	5.32	2.83	6.55	4.73	6.50	−1.2	0.6	−3.7	4.3	1.59	1.16	1.48
Garnets															
Fe_{16}	19	1713	927	4.71	2.70	7.89	6.84	4.89	−3.1	−2.1	−2.2	0.1	1.85	1.05	1.38
Fe_{36}	19	1682	922	4.71	2.67	7.42	5.98	5.05	−2.7	−1.3	−2.4	1.1	1.82	1.01	1.37
Fe_{54}	24	1736	955	5.38	2.52	6.79	5.52	4.81	−1.3	−0.1	−2.3	2.2	1.82	1.28	1.37
$MgAl_2O_4$	21	1969	1080	4.85	0.92	5.47	3.84	4.19	−0.6	1.0	−3.3	4.3	1.82	1.40	0.67
$SrTiO_3$	25	1741	1168	5.67	3.92	11.2	8.77	8.70	−5.3	−3.1	−4.8	1.7	1.49	1.63	1.06
$KMgF_3$	60	751	488	4.87	2.98	5.02	3.46	4.72	−0.0	1.4	−1.7	3.1	1.54	1.60	1.50
$RbMnF_3$	57	675	341	4.80	3.69	4.48	3.01	5.04	0.4	1.8	−1.4	3.1	1.98	1.49	1.80
$RbCdF_3$	40	614	257	1.09	2.15	4.12	3.06	3.27	−3.0	−2.0	−1.1	−0.8	2.39	1.06	0.80
$TlCdF_3$	49	609	228	7.43	0.95	5.09	3.86	3.14	2.4	3.6	−2.2	5.8	2.68	1.24	1.03
ZnO	15	1394	442	4.76	−2.2	9.60	6.22	3.02	−4.8	−1.5	−5.2	3.7	3.15	0.81	−0.4
BeO	18	2201	1618	5.48	1.19	5.17	3.08	4.19	0.3	2.4	−3.0	5.4	1.36	1.27	0.79
SiO_2	35	378	455	6.37	0.35	3.28	2.43	−0.3	3.1	3.9	0.7	3.3	0.85	0.67	0.40
$CaCO_3$	17	747	318	5.36	−3.5	24.0	23.1	18.5	−19	−18	−22	4.2	2.35	0.56	−1.0

TABLE 6-8
Dimensionless Logarithmic Anharmonic Derivatives

Substance	$\{K_S\}_T$	$\{G\}_T$	$\{K_S\}_P$	$\{G\}_P$	$\{K_S\}_V$	$\{G\}_V$
Averages						
Halides	5.1	2.6	4.1	5.9	0.9	−3.3
Perovskites*	4.8	2.7	4.4	5.0	0.3	−2.2
Garnets*	4.9	2.6	6.1	4.9	−1.2	−2.3
Fluorites*	5.0	2.2	4.8	5.2	0.2	−2.9
Oxides	5.3	2.0	5.7	5.8	−0.4	−3.7
Silicates	5.6	2.8	5.4	5.4	0.2	−2.6
Grand	5.1 (±1.0)	2.5 (±1.3)	5.0 (±1.9)	5.7 (±1.9)	0.1 (±1.9)	−3.2 (±1.9)
Olivine	5.1	2.9	4.9	6.7	0.2	−3.8
Olivine	4.8	2.9	4.7	6.3	0.2	−3.4
$MgAl_2O_4$-spinel	4.9	0.9	3.8	4.2	−0.6	+1.0

$\{M\} = \partial \ln M / \partial \ln \rho$

*Structures.

$$(\partial \ln V_p/\partial \ln \rho) = \frac{1}{2}\left[\frac{3}{5}(\partial \ln K_S/\partial \ln \rho) + \frac{2}{5}(\partial \ln G/\partial \ln \rho) - 1\right]$$

where we have used $K_S = 2G$, a value appropriate for the lower mantle. For "typical" laboratory values, $\delta_S = 4$, $g = 6$, we would have $(\partial \ln V_p/\partial \ln \rho)_P = 1.9$. For comparison, if $\partial \ln V_s = 2\,\partial \ln V_p$ and 6, $= 4$, we would have $(6 \ln V_p/\delta \ln \rho)_P = 4.5$, which is much greater than observed for the lower mantle.

Seismic tomography has recently established that $d \ln V_s \approx 2\, d \ln V_p$ for the lateral variations in velocity in the lower mantle (Woodhouse and Dziewonski). This implies that lateral variations in rigidity are much greater than lateral variations in bulk modulus. The value of $(\partial \ln V_p/\partial \ln \rho)_P$ can be used to establish the following bounds:

$$\{G\}_P \equiv (\partial \ln G/\partial \ln \rho)_P < 8.5$$

$$\{K_S\}_P \equiv (\partial \ln K_S/\partial \ln \rho)_P < 5.7$$

for K, $= 2G$. If G and K contribute equally, the normalized derivatives would be about 3.4. The numerical factors in the above equations are very insensitive to K_S/G.

By combining the relations obtained from tomography and the geoid we obtain

$$\{K_S\}_P \equiv \delta_S = (\partial \ln K_S/\partial \ln \rho)_P = (K_S\alpha)^{-1}(\partial K_S/\partial T)_P = 1.8$$

$$\{G\}, \equiv g = (\partial \ln G/\partial \ln \rho)_P = (G\alpha)^{-1}(\partial G/\partial T)_P = 5.8$$

The former is about one-fourth of normal laboratory values of 6, taken at modest temperature and pressure, values which are dominated by the extrinsic component. A reduction of this order is consistent with the expected decrease with pressure and implies that the extrinsic component, although greatly reduced, still dominates in the lower mantle.

On the other hand, the value for g is comparable to laboratory values for most materials and within 30 percent of close-packed oxides such as Al_2O_3 and $SrTiO_3$. The intrinsic component apparently represents a large fraction of the total temperature effect. The above value for g is about twice the extrinsic contribution typical of close-packed silicates and oxides, again suggesting an important intrinsic effect.

The Griineisen Parameters of the Lower Mantle

The thermodynamic *Grüneisen* parameter is defined as

$$\underline{\gamma} = \alpha K_T/\rho C_V = \alpha K_S/\rho C_P$$

This parameter generally has a value between 1 and 2 for materials of geophysical interest and is approximately constant at high temperature. On the other hand it varies with volume, but the volume dependency appears to decrease with compression (Birch, 1961). The parameter $\underline{\gamma}$ is important in temperature-dependent equations of state. For example the thermal or vibrational pressure is

$$P^* = \alpha K_T T = (C_V \underline{\gamma}/V)T$$

and the differential form of the Mie-Griineisen equation of state is

$$(\partial P/\partial T)_V = \underline{\gamma}\rho C_V$$

Brillouin (1964) considered the vibrational pressure to be due to the radiation pressure of diffuse elastic waves. By

TABLE 6-9
Anharmonic Parameters for Oxides and Silicates and Predicated Values for Some High-pressure Phases

Mineral	$\{K_T\}_T$	$\{K_S\}_T$	$\{G\}_T$	$\{K_T\}_P$	$\{K_S\}_P$	$\{G\}_P$
a-olivine	5.0	4.8	2.9	6.6	4.7	6.5
β-spinel*	4.9	4.8	3.0	6.6	4.7	6.4
y-spinel*	5.1	5.0	3.1	6.8	4.9	6.5
Garnet	4.8	4.7	2.7	7.9	6.8	4.9
$MgSiO_3$ (majorite)*	4.9	4.7	2.6	7.9	6.0	4.5
Al_2O_3-ilmenite	4.4	4.3	2.7	6.8	4.3	7.5
$MgSiO_3$-ilmenite*	4.7	4.5	2.7	7.0	4.3	6.0
$MgSiO_3$-perovskite*	4.5	4.5	3.5	7.5	5.5	6.5
*	4.2	4.1	2.8	6.2	4.0	5.7
SiO_2 (stishovite)*	4.5	4.4	2.4	7.5	6.4	5.0

*Predicted.

ignoring dispersion and the optical modes it is possible to estimate γ from macroscopic elastic measurements. This yields the Brillouin or acoustic Griineisen parameter γ_{BR}.

In the Grüneisen-Debye theory of the equation of state, the Griineisen ratio for a given mode is written

$$\gamma = -\frac{\mathrm{d} \ln \theta}{\mathrm{d} \ln V} = -\frac{\mathrm{d} \ln \nu_m}{\mathrm{d} \ln V}$$

where ν_m is the maximum lattice vibration frequency and 8 is the Debye temperature. In an isotropic solid we have one ν_m for the longitudinal modes and a different one for the two shear modes. The acoustic or Brillouin-Griineisen ratio (Mnopoff, 1963; Brillouin, 1964) can be written

$$\gamma_{BR} = -\frac{1}{6} + \frac{1}{2}\left(\frac{\mathrm{d} \ln K}{\mathrm{d} \ln \rho}\right)_T - \frac{1}{3}\left(\frac{\mathrm{d} \ln f(\sigma)}{\mathrm{d} \ln \rho}\right)_T$$

where $f(\sigma)$ is a function of Poisson's ratio, σ, or KIG. The expression involving this term is assumed in classical theory (previous sections) to be zero, implying that all elastic constants have the same pressure or volume dependence. This is clearly not a good approximation for silicates or the Earth's mantle. In our notation the acoustic γ can be written (with K = K_T)

$$\gamma = \frac{1}{2}\left(\frac{\partial \ln K}{\partial \ln \rho}\right)_T - \frac{1}{6} - [(\mathrm{KIG}) + 2][3(K/G) + 4]^{-1} \times \left[\left(\frac{\partial \ln K}{\partial \ln \rho}\right)_T - \left(\frac{\partial \ln G}{\partial \ln \rho}\right)_T\right] \quad (15)$$

which reduces to the classical form when

$$\left(\frac{\partial \ln K}{\partial \ln \rho}\right)_T = \left(\frac{\partial \ln G}{\partial \ln \rho}\right)_T$$

In the lower mantle K $\approx 2G$, and we have

$$\gamma = \frac{1}{2}\left(\frac{\partial \ln K}{\partial \ln \rho}\right)_T - \frac{1}{6} - \frac{2}{5}\left[\left(\frac{\partial \ln K}{\partial \ln \rho}\right)_T - \left(\frac{\partial \ln G}{\partial \ln \rho}\right)_T\right] \quad (16)$$

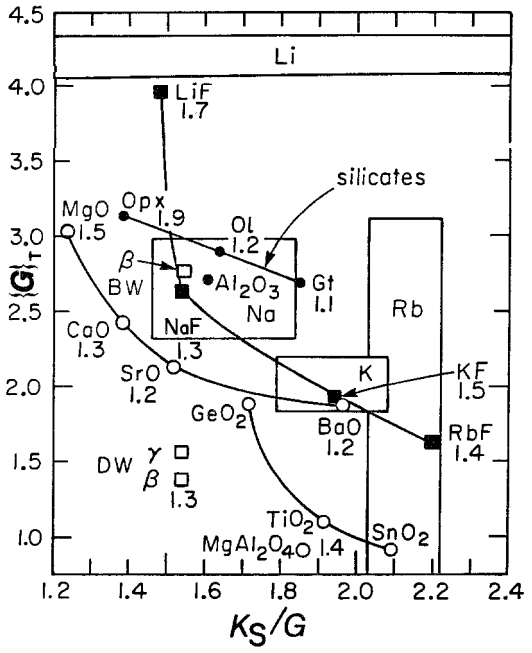

FIGURE **6-3**
$\{G\}_T = (\partial \ln G/\partial \ln \rho)_T$ versus K_S/G for oxides, silicates, and halides (Opx = orthopyroxene, 01 = olivine, Gt = garnet). Boxes enclose measurements for Li, Na, K and Rb rocksalt halides. Parameter (numerals) is the Griineisen parameter y. Open squares are DW and BW parameters for β-spinel (from D. Weidner, 1987 and Bina and Wood, 1987, respectively). The curves connect the oxide rutiles, rocksalt oxides, silicates and the fluorides.

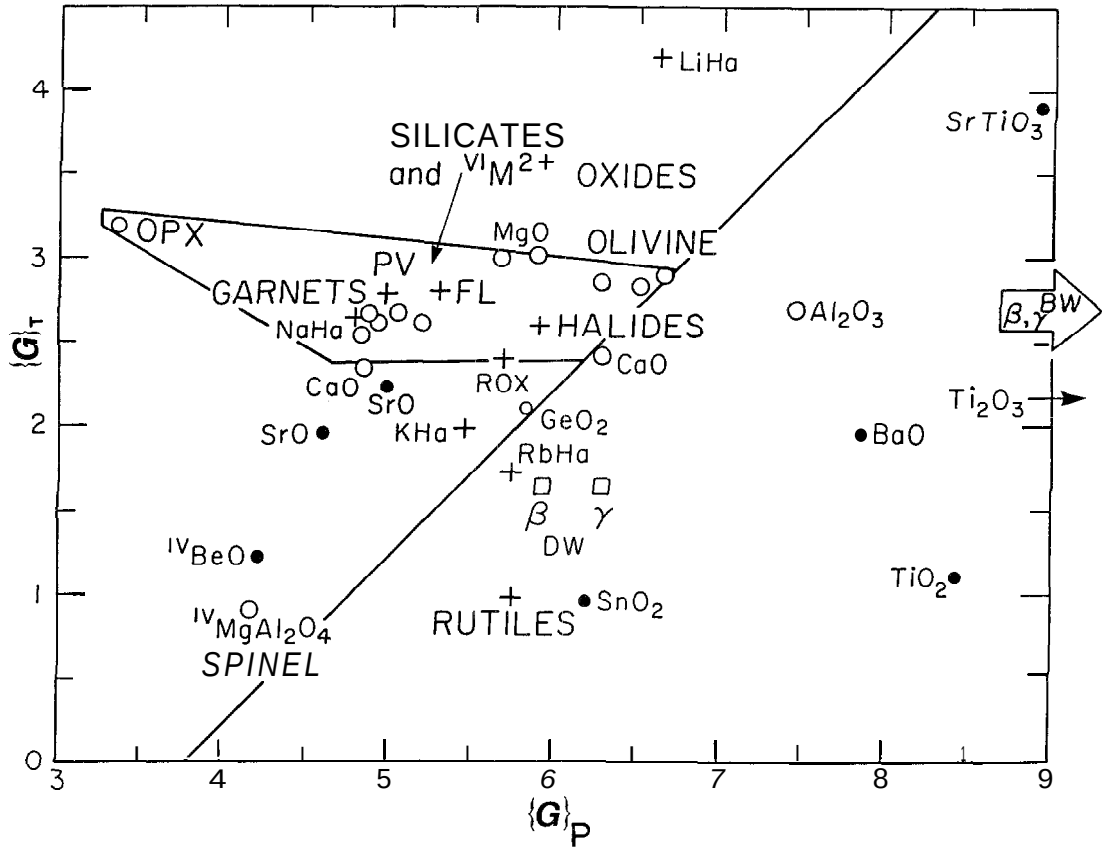

FIGURE 6-4
{G}, versus {G}, for various crystals. Symbols and sources same as for Figure 6-3.

The variation of rigidity dominates this expression. For lower-mantle values we obtain y = *1.2* ± *0.1* and, for extrapolated zero-pressure values, $\gamma_o = 1.4$. The numerical factor 2/5 is remarkably insensitive to variations in *KIG*, and equation *16* therefore has wide generality. The near cancellation of the bulk modulus terms means that the correction from adiabatic seismic properties to the high-frequency isothermal properties appropriate for lattice vibrations is very small.

The Griineisen ratio can also be written:

$$\gamma = -(\partial \ln T/\partial \ln V)_S = K_S(\partial \ln T/\partial P)_S$$

For the adiabatic gradient at 1000 km depth we obtain $(\partial \ln T/\partial P)_S = 3.3 \times 10^{-4}$/kbar and twice this at the zero-pressure extension of the lower-mantle adiabat. The latter is 0.44°C/km for $T_o = 1700\ K$. The absolute temperature along the adiabat increases by about *22* percent from zero pressure to 1000 km depth, giving T_S *(1000* km) = *2080* K for $T_o = 1700\ K$.

The Griineisen parameter is related to thermal pressure, thermal expansion, and other anharmonic properties. Thermal or internal pressure is caused by diffuse elastic waves that expand the lattice. Thermally generated compressional and shear waves contribute to this internal pressure, which affects the elastic moduli at finite temperature. The Griineisen parameter can therefore be estimated either from the thermal properties or from the volume dependence of the elastic moduli. The so-called acoustic, elastic or non-thermal Griineisen parameter usually shows poor agreement with the thermal y, and various attempts have been made to patch up the theory connecting these parameters to obtain better agreement. A common assumption in most theories is that the moduli or the elastic velocities have the same volume dependence at constant temperature. If so, y can be estimated from the pressure dependence of one of the moduli. For example, the Slater value, γ_{SL}, is

$$\gamma_{SL} = \frac{1}{2}\left[\frac{\partial \ln K}{\partial \ln \rho}\right]_T - \frac{1}{6} = \frac{1}{2}\left(\frac{\partial K}{\partial P}\right)_T - \frac{1}{6} \qquad (17)$$

This is derived from Debye's model of coupled atomic vibrations. If the atoms in a solid behave independently, we have the Druyvesteyn and Meyering or Dugdale and MacDonald (DM) value

$$\gamma_{DM} = \gamma_{SL} - \frac{1}{3}$$

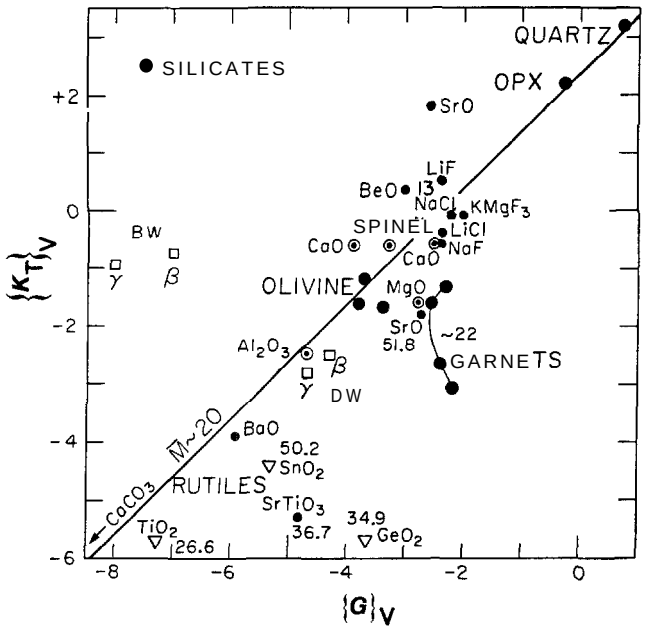

FIGURE 6-5
Intrinsic derivatives $\{K_T\}_V$ versus $\{G\}_V$. Most oxides and silicates with mean atomic weight ($\overline{M}$) near 20 ($CaCO_3$, Al_2O_3, olivine, spinel, orthopyroxene and quartz) fall near the line. Crystals with transition-element cations and high $\overline{M}$ fall below the line. The points for CaO and SrO help to indicate the scatter in presently available data. The open squares are the values adopted by BW (Bina and Wood, 1987) and DW (D. Weidner, 1987) for the spinel forms of Mg_2SiO_4. The numbers are $\overline{M}$, mean atomic weight.

The free-volume γ is, at zero pressure,

$$\gamma_{FV} = \gamma_{SL} - \frac{2}{3}$$

Equation 15 is derived with less restrictive assumptions and it shows the importance of the volume dependence of the rigidity. The rigidity, a factor in both the compressional and shear waves, plays the more important role.

The various y's are computed for a variety of crystals and summarized in Table 6-10. The values in this table are computed from data reported in Sumino and Anderson (1984), Jones (1979) and Bohler (1982). γ_{BR} is calculated from equation 15. The factor involving K/G is nearly a constant, ranging only from 0.39 to 0.42 for KIG from 2.5 to 1.2. Most crystals relevant to geophysics exhibit an even smaller range of KIG. Therefore, a simpler form is

$$\gamma_A = \frac{1}{10}\left(\frac{\partial \ln K}{\partial \ln \rho}\right)_T + \frac{4}{10}\left(\frac{\partial \ln G}{\partial \ln \rho}\right)_T - \frac{1}{6}$$

and this is tabulated as well.

The dominance of the rigidity suggests an even simpler approximation,

$$\gamma_G = \frac{1}{2}\left(\frac{\partial \ln G}{\partial \ln \rho}\right)_T - \frac{1}{6}$$

which ignores the bulk modulus data altogether. γ_G and γ_{SL} bound γ for most ionic crystals. γ_G is closer to $\gamma_{thermal}$ than the γ's derived from $(\partial \ln \mathrm{Kld} \ln \rho)_T$ alone, even those involving elaborate refinements in the theory. The assumption that the volume dependence of the rigidity is the same as that of the bulk modulus is the most serious shortcoming of conventional lattice dynamic γ's such as the Slater and the free-volume forms. In general,

$$[\partial \ln G/\partial \ln \rho]_T < [\partial \ln \mathrm{Kla} \ln \mathrm{p}],$$

Various approximations must be made in the determination of the acoustic y, and there are also uncertainties in the pressure derivatives of the elastic moduli. Further uncertainties are introduced by the methods of averaging the elastic properties and their derivatives when computing γ for anisotropic crystals. This makes it difficult to compare the acoustic and thermodynamic γ's and to assess the importance of high-frequency and optical modes. O. L. Anderson (1986) argued that y nearly equals the thermodynamic γ for dense, close-packed minerals and therefore for the lower mantle. The neglect of shear-mode data and the assumption that all acoustic modes share the same volume dependence are the most serious shortcomings of most attempts to compare γ with γ. Experimental uncertainties in

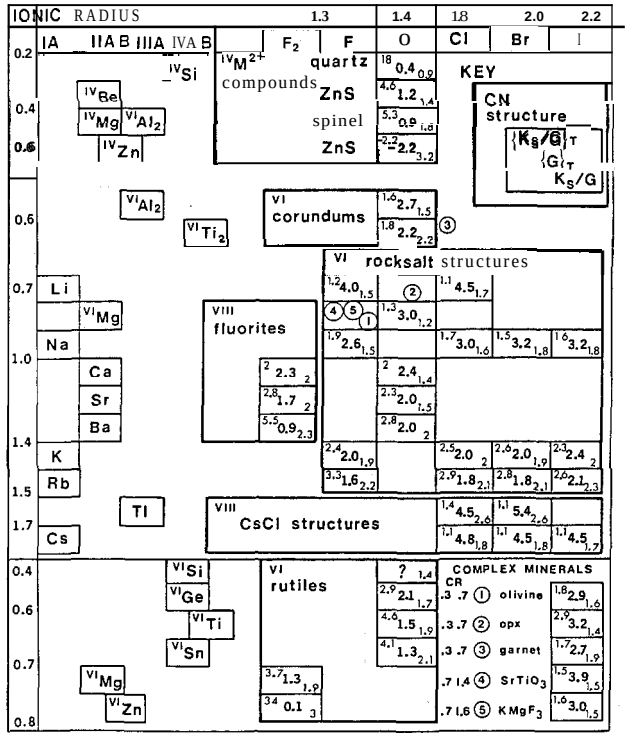

FIGURE 6-6
The shear properties of simple ionic crystals arranged by anion and cation radius. The circled numbers indicate the approximate location appropriate for the more complex ionic crystals (lower right). Note the trends with cation and anion radius. CN, cation coordination.

TABLE 6-10
Comparison of Grüneisen Parameters

Parameter	MgO	Al_2O_3	OLIVINE	GARNET	$SrTiO_3$	$KMgF_3$
$(\partial \ln K/\partial \ln \rho)_T$	3.80	4.34	4.83	4.71	5.67	4.87
$(\partial \ln G/\partial \ln \rho)_T$	3.01	2.71	2.85	2.67	3.92	2.99
K/G	1.24	1.54	1.59	1.82	1.49	1.54
γ_{SL}	1.73	2.00	2.25	2.19	2.67	2.27
γ_{DM}	1.40	1.67	1.92	1.86	2.34	1.94
γ_{FV}	1.06	1.33	1.58	1.52	2.00	1.60
γ_G	1.34	1.19	1.26	1.17	1.79	1.33
γ_{BR}	1.40	1.33	1.43	1.37	1.95	1.50
γ_A	1.40	1.35	1.46	1.37	1.97	1.52
$\gamma_{thermal}$	1.55	1.33	1.18	1.20	1.86	1.83
	1.39		1.23	1.37		
$\frac{(K/G)+2}{3(K/G)+4}$	0.42	0.41	0.41	0.40	0.41	0.41

$\gamma_{SL} = \frac{1}{2}(\partial \ln K/\partial \ln \rho)_T - 1/6$ *(Slater value)*

$\gamma_{DM} = \gamma_{SL} - 1/3$ (Druyvesteyn *and* Meyering *or* Dugdale *and* MacDonald *value)*

$\gamma_{FV} = \gamma_{SL} - 2/3$ *(free-volume value)*

$\gamma_G = \frac{1}{2}(\partial \ln G/\partial \ln \rho)_T - 1/6$ *(rigidity-based approximation)*

$\gamma_{BR} = \gamma_{SL} - [(K/G)+2]\,[3(K/G)+4]^{-1}\left[\left(\frac{\partial \ln K}{\partial \ln \rho}\right)_s - \left(\frac{\partial \ln G}{\partial \ln \rho}\right)_s\right]$ (Brillouin *or acoustic value)*

$\gamma_A = \gamma_{SL} - 2/5\left[\left(\frac{\partial \ln K}{\partial \ln \rho}\right)_s - \left(\frac{\partial \ln G}{\partial \ln \rho}\right)_s\right]$ *(simplified* γ_{BR}*)*

$\gamma_{thermal} = \alpha K_T/\rho C_V$

the pressure derivatives, particularly K'_T, complicate the situation further. The acoustic y, of course, does not include the contribution of the optical modes.

Thermodynamics of the Lower Mantle

The relative change in the variation of shear velocity in the radial (depth) direction is about 0.7 times that of the compressional velocity. On the other hand, the lateral variation of relative shear velocity is about 2 times the compressional variation. This immediately indicates that the elastic moduli are not the same function of volume and that there is an intrinsic temperature effect over and above the effect of volume. The above relations can be interpreted as

$$\left(\frac{\partial \ln V_s}{\partial \ln V_p}\right)_T = 0.7$$

$$\left(\frac{\partial \ln V_s}{\partial \ln V_p}\right)_P = 2.0$$

The relationship between V_p and V_s variations for the lower-mantle value of K = 2G is

$$1 + 2(\mathrm{d} \ln V_p/\partial \ln \rho)_P = (3/5)\delta_S + (215)(1 + 2\,\partial \ln V_s/\partial \ln \mathrm{p}), \quad (18)$$

Here again the numerical factors are insensitive to K_S/G. Assuming a range of $\mathrm{d} \ln V_s$ = (2 to 2.5) $\mathrm{d} \ln V_p$ for lateral variations and attributing these to temperature we have

$$\delta_S = 1.8 \text{ to } 1.0$$

This is much lower than the range 4 to 6 that is typical of oxides under laboratory conditions and lower than the lower-mantle K'_S, which ranges from 3.0 to 3.8. Furthermore, using the value $(\mathrm{d} \ln V_p/\partial \ln \mathrm{p}), = 1.2$ inferred above from the tomography-geoid correlation (Hager and others, 1985), we have

$$(\partial \ln V_s/\partial \ln \mathrm{p}), = 2.4 \text{ to } 3.0$$

giving

$$g = (\partial \ln G/\partial \ln \mathrm{p}), = 5.8 \text{ to } 7.0$$

and, for completeness,

$$6, = (\partial \ln K_S/\partial \ln \rho)_P = 1.8 \text{ to } 1.0$$

From PREM we have

$$(\partial \ln G/\partial \ln \rho)_S = 2.4 \text{ to } 2.6$$

$$(\partial \ln K_S/\partial \ln \rho)_S = 3.0 \text{ to } 3.8$$

This shows that the elastic constants are not strictly a function of volume and that lateral variations in rigidity

are much more important than lateral variations in bulk modulus. Derivatives along the adiabat ($d \ln M/\partial \ln p$), differ slightly from the corresponding isothermal derivatives. ($\partial \ln K_S/\partial \ln p$), is within 2 percent of ($\partial \ln K_S/\partial \ln \rho)_S$. On the other hand ($\partial \ln G/\partial \ln p$), is 4 to 16 percent higher than ($\partial \ln G/\partial \ln p$),, and this correction is important in modeling and interpreting seismic data in terms of chemistry and mineralogy.

We can also obtain some information on the coefficient of thermal expansion, a , in the lower mantle. Using the thermodynamic identity

$$\left(\frac{\partial \alpha}{\partial \ln V}\right)_T = -\left(\frac{\partial \ln K_T}{\partial T}\right)_P$$

we can write

$$\left(\frac{\partial \ln \alpha}{\partial \ln V}\right)_T = -\left(\frac{\partial \ln K_T}{\partial \ln V}\right)_P = \delta_T \qquad (19)$$

Since

$$\delta_T \approx \delta_S + \gamma$$

according to equation 12, then

$$-\left(\frac{\partial \ln \alpha}{\partial \ln \rho}\right)_T = \delta_S + \gamma$$

$$\simeq 3.1 \text{ to } 2.1$$

using values found previously. High-temperature data on NaCl and KC1 (Yamamoto and Anderson, 1986) suggest an increase of about 10 percent in these values since 6, $-\delta_S$ is slightly greater than y. Therefore a is inversely proportional to density to about the second or third power in the lower mantle. This causes a substantial reduction in a . From the Grüneisen relation and the extrapolated values from PREM for the lower mantle, we obtain $a, = 3.8 \times 10^{-5}/K$ for zero pressure and high temperature. This is almost identical to the high-temperature value for $MgSiO_3$-perovskite (Knittle and others, 1986).

The volume dependence of γ is of both theoretical and practical importance since γ needs to be known at high pressure in order to interpret shock-wave and seismic data. The variation of thermodynamic γ with p at constant temperature is

$$q = \left(\frac{\partial \ln \gamma}{\partial \ln \rho}\right)_T = \left(\frac{\partial \ln \alpha}{\partial \ln \rho}\right)_T + \left(\frac{\partial \ln K_T}{\partial \ln \rho}\right)_T - \left(\frac{\partial \ln C_V}{\partial \ln \rho}\right)_T - 1 \qquad (20)$$

At this point it is common to perform some thermodynamic manipulations and then to make some approximations and to assume that one or more derivations can be set to zero. For example,

$$\left(\frac{\partial \ln \gamma}{\partial \ln \rho}\right)_T \simeq \frac{1}{\alpha}\left(\frac{\partial \ln K_S}{\partial T}\right)_V - 1 - \gamma$$

if C_V is constant, $\alpha\gamma T \ll 1$, $(\partial\alpha/\partial T)_V = 0$ and $(\partial\gamma/\partial T)_V = 0$. With the parameters derived for the lower mantle,

$$\left(\frac{\partial \ln \gamma}{\partial \ln \rho}\right)_T \simeq 0 \pm 1$$

A different approximation is

$$\left(\frac{\partial \ln \gamma}{\partial \ln \rho}\right)_T = (1 + \alpha\gamma T)^{-1}\left[\frac{1}{\alpha}\left(\frac{\partial \ln K_S}{\partial T}\right)_V - 1 - \gamma - \alpha\gamma T\left(\frac{\partial \ln K_S}{\partial \ln \rho}\right)_P\right]$$

where $(\partial\gamma/\partial T)_P$ has been set to zero (Bassett and others, 1968). This gives

$$\left(\frac{\partial \ln \gamma}{\partial \ln \rho}\right)_T \simeq -0.5 \pm 1$$

The above estimates are consistent with a constant γ or a weak variation with depth. The usual approximation

$$q = \left(\frac{\partial \ln \gamma}{\partial \ln \rho}\right)_T = -1$$

is based on the assumption that C_V is independent of volume at constant temperature and $(\partial K_T/\partial T)_V$ is zero or αK_T is independent of volume and temperature.

The approximations with the strongest experimental support, at high temperature, are

$$(\partial \alpha K_T/\partial T)_P \simeq 0$$

$$(\partial \alpha/\partial T)_V \simeq 0$$

$$(\partial K_T/\partial T)_V \simeq 0$$

Our estimate of $\frac{1}{a}\left(\frac{\partial \ln K_S}{\partial T}\right)_V$ for the lower mantle is o n - sistent with

$$\frac{1}{\alpha}\left(\frac{\partial \ln K_T}{\partial T}\right)_V \simeq 0$$

since

$$\frac{1}{\alpha}\left(\frac{\partial \ln K_S}{\partial T}\right)_V \simeq \frac{1}{\alpha}\left(\frac{\partial \ln K_T}{\partial T}\right)_V + \gamma$$

The derivative $(\partial\gamma/\partial T)_P$ is close to zero, but $(\partial\gamma/\partial T)_V$ is negative. Theoretically, $(\partial \ln C_V/\partial \ln V)_S$ should be very small.

With these relations in mind we write:

$$\left(\frac{\partial \ln \gamma}{\partial \ln \rho}\right)_S = \left(\frac{\partial \ln \alpha}{\partial \ln \rho}\right)_S + \left(\frac{\partial \ln K_T}{\partial \ln \rho}\right)_S - \left(\frac{\partial \ln C_V}{\partial \ln \rho}\right)_S - 1$$

$$= \frac{K_S}{K_T}\left[\frac{1}{\alpha}\left(\frac{\partial \ln K_T}{\partial T}\right)_V\right] + \alpha\left(\frac{\partial \ln \alpha}{\partial \ln T}\right)_P$$

$$+ \gamma\left(\frac{\partial \ln K_T}{\partial \ln T}\right)_P - \left(\frac{\partial \ln C_V}{\partial \ln \rho}\right)_S - 1$$

$$= \frac{K_S}{K_T}\left[\frac{1}{\alpha}\left(\frac{\partial \ln K_T}{\partial T}\right)_V\right] + \gamma T\left(\frac{\partial \ln \alpha}{\partial T}\right)_V - \left(\frac{\partial \ln C_V}{\partial \ln \rho}\right)_S - 1$$

$$\simeq -1$$

Now

$$\left(\frac{\partial \ln \gamma}{\partial \ln \rho}\right)_S = \frac{K_S}{K_T}\left(\frac{\partial \ln \gamma}{\partial \ln \rho}\right)_T + \gamma\left(\frac{\partial \ln \gamma}{\partial \ln T}\right)_P$$

$$= \left(\frac{\partial \ln \gamma}{\partial \ln \rho}\right)_T + \gamma T\left(\frac{\partial \ln \gamma}{\partial T}\right)_V$$

Therefore, $|(\partial \ln \gamma/\partial \ln \rho)_S| > |(\partial \ln \gamma/\partial \ln \rho)_T|$. Since $K_S > K_T$, $(\partial \ln \gamma/\partial \ln T) \simeq 0$ and $(\partial \ln \gamma/\partial T)_V < 0$,

$$q = \left(\frac{\partial \ln \gamma}{\partial \ln \rho}\right) = -1 + \varepsilon$$

The parameter q itself depends on compression. Model calculations show that the absolute value of q decreases with compression, meaning that γ should be only a weak function of density in the lower mantle (Hardy, 1980). The seismic data are therefore consistent with theoretical expectations.

Although extrinsic effects are suppressed by pressure, they are enhanced at high temperature. This permits us to estimate the effect of temperature on K'_S and G'. From PREM parameters for the lower mantle, we have

$$(\partial \ln M'/\partial \ln \rho) \approx -1$$

where M' is K' or G'. Assuming a mean atomic weight of 21, we derive, for the lower mantle,

$$K'_S = 0.78V_m$$

where V_m is the mean molar volume. This relation also satisfies ultrasonic K'_S versus V_m data for olivines, garnets, $SrTiO_3$-perovskite and MgF_2-rutile and predicts K'_S to within about 10 percent for Al_2O_3, MgO and CaO. If these relations also hold for a change in temperature, then

$$\partial K'_S/K'_S \simeq -\partial\rho/\rho = \alpha\partial T$$

and K'_S at 1700 K is predicted to be about 6 percent higher than K'_S at 300 K. This is more important than the difference between K'_S and K'_T.

Summary of Lower-Mantle Thermodynamics

Assuming that the lower mantle is adiabatic and chemically homogeneous, it is possible to obtain reliable estimates of lower-mantle properties extrapolated to zero pressure and high temperature (Butler and Anderson, 1978; Jeanloz and Knittle, 1986). (The temperature correction is described in the next section.) These extrapolations provide evidence that the lower mantle is predominantly perovskite and that it differs from the inferred composition of the upper mantle. Representative extrapolated values for the lower mantle are

$$\rho_o = 3.97\text{–}4.00\ \text{g/cm}^3$$

$$K_o = 2.12\text{–}2.23\ \text{kbar}$$

$$G_o = 1.30\text{–}1.35\ \text{kbar}$$

$$(K'_o)_S = 3.8\text{–}4.1$$

$$(G'_o)_S = 1.5\text{–}1.8$$

The entire lower mantle is not radially homogeneous. The region between about 650 and 750 km has high gradients of seismic velocity, probably due to a mixed-phase region involving y-spinel and majorite transforming to ilmenite and perovskite. The seismic results may also be sensing a deflection of the 650-km seismic discontinuity. The lowermost 200 to 300 km of the mantle, region D", is also radially and laterally inhomogeneous.

The lowermost mantle is probably the dumping ground for light material exsolving from the core and ancient relict dense phases subducted while the Earth was accreting. It is therefore probably a chemically distinct layer composed of dense refractory silicates. Superposed on this is the high thermal gradient in the mantle-core thermal boundary layer. It has previously been supposed that the thickness of D" is too great for it to be simply a thermal boundary, but the considerations in this section, particularly the decrease with rising pressure of the coefficient of thermal expansion and the large increase in the lattice thermal conductivity, show that a thick thermal boundary is likely. The low a, the high conductivity and the possibility of an intrinsic high density will tend to stabilize this layer until a large temperature gradient is built up. It may, however, accommodate small-scale convection, which will contribute to the observed lateral variability in seismic properties and, possibly, thickness. The transition zones at the top and bottom of the lower mantle are excluded from the present analysis.

The radial and lateral variation of seismic velocities in the mantle can be used to estimate important thermodynamic properties and to test some standard equation-of-state assumptions. The radial variations yield K' and G', which are related to $(\partial \ln K_S/\partial \ln \rho)_T$ and $(\mathrm{d} \ln G/\partial \ln \rho)_T$ and the corresponding values along an adiabat. These in turn are related to the volume-dependent or extrinsic effects of temperature. The lateral variations, if due to temperature, yield estimates of derivatives at constant pressure, that is, δ_S and G. These derivatives are closely connected to the Grüneisen parameters y and 6. Theoretically, the effects of temperature decrease with compression, and this is borne out by the seismic data. In the lower mantle the lateral variation of seismic velocities is dominated by the effect of temperature

on the rigidity. This is similar to the situation in the upper mantle except that there it is caused by nonelastic processes, such as partial melting and dislocation relaxation, phenomena accompanied by increased attenuation. In the lower mantle the effect is caused by anharmonic phenomena and intrinsic temperature effects that are more important in shear than in compression. One cannot assume that physical properties are a function of volume alone, that classical high-temperature behavior prevails, or that shear and compressional modes exhibit similar variations. On a much more basic level, one cannot simply adopt laboratory values of temperature derivatives to estimate the effect of temperature on density and elastic-wave velocities in slabs and in the deep mantle.

From the seismic data for the lower mantle, we obtain the following estimates of in-situ values:

$$(\partial \ln G/\partial \ln \rho)_P \quad 5.8 \text{ to } 7.0$$

$$(\partial \ln G/\partial \ln \rho)_T \quad 2.6 \text{ to } 2.9$$

$$(\partial \ln K_S/\partial \ln \rho)_P \quad 1.8 \text{ to } 1.0$$

$$(\partial \ln K_S/\partial \ln \rho)_T \quad 2.8 \text{ to } 3.6$$

$$(d \ln \gamma/\partial \ln \rho)_T \quad -1 + \varepsilon$$

$$-(\partial \ln \alpha/\partial \ln \rho)_T \quad 3 \text{ to } 2$$

For the intrinsic temperature terms we obtain:

$$\frac{1}{\alpha}\left[\frac{\partial \ln G}{\partial T}\right]_V \approx -3.2 \text{ to } -4.1$$

$$\frac{1}{\alpha}\left[\frac{\partial \ln K_S}{\partial T}\right]_V \approx +1 \text{ to } +2.6$$

The former is in the range of laboratory measurements. The latter is positive, indicating that an increase of temperature at constant volume causes K_S to increase. It can be compared with the value of $+1.4$ found for $KMgF_3$-perovskite. From lower-mantle values extrapolated to the surface, we obtain $a, = 3.8 \times 10^{-5}$/K and $\gamma_o = 1.43$. These are very close to estimates of Birch (1968).

An interesting implication of the seismic data is that the bulk modulus and rigidity are similar functions of volume at constant temperature. On the other hand, G is a stronger function of volume and K_S a much weaker function of volume at constant pressure than they are at constant temperature.

CORRECTING ELASTIC PROPERTIES FOR TEMPERATURE

The elastic properties of solids depend primarily on static lattice forces, but vibrational or thermal motions become increasingly important at high temperature. The resistance of a crystal to deformation is partially due to interionic forces and partially due to the radiation pressure of high-frequency acoustic waves, which increase in intensity as the temperature is raised. If the increase in volume associated with this radiation pressure is compensated by the application of a suitable external pressure, there still remains an intrinsic temperature effect. Thus,

$$K(V,T) = K(V,0) + K(\partial \ln K/\partial T)_V T \qquad (21)$$

$$G(V,T) = G(V,0) + G(\partial \ln G/\partial T)_V T \qquad (22)$$

These equations provide a convenient way to estimate the properties of the static lattice, that is, $K(V,0)$ and $G(V,0)$, and to correct measured values, $K(V,T)$ and $G(V,T)$, to different temperatures at constant volume. The static lattice values should be used when searching for velocity-density or modulus-volume systematics or when attempting to estimate the properties of unmeasured phases. These equations can also be used to correct laboratory or seismological data in forward or inverse modeling of mantle properties. The correction to a different or standard volume, at constant temperature, involves the extrinsic derivatives $(\partial \ln Mid \ln p)$,.

The first step in forward modeling of the seismic properties of the mantle is to compile a table of the ambient or zero-temperature properties, including temperature and pressure derivatives, of all relevant minerals. The fully normalized extrinsic and intrinsic derivatives are then formed and, in the absence of contrary information, are assumed to be independent of temperature. The coefficient of thermal expansion, $\alpha(T)$ or $\alpha(\theta/T)$, can be used to correct the density to the temperature of interest at zero pressure. It is important to take the temperature dependence of $\alpha(T)$ into account properly since $\alpha(T)$ increases rapidly from room temperature but levels out at high T/θ. The use of the ambient a, will underestimate the effect of temperature; the use of a, plus the initial slope, $(\partial\alpha/\partial T)_o$ in a linear approximation, will overestimate the volume change at high temperature. Fortunately, the shape of $\alpha(T)$ is well known theoretically (a Debye function) and has been measured for many mantle minerals (see Table 6-7). The moduli can then be corrected for the volume change using $(\partial \ln M/\partial \ln p)$, and corrected for temperature using $(\partial \ln M/\partial T)_V$. The parameters $(\partial \ln M/\partial \ln p)$, or $(\partial \ln Mld \ln p)$, are then used in an equation of state to calculate $M(P,T)$, for example, from finite strain. The normalized form of the pressure derivatives can be assumed to be either independent of temperature or functions of $V(T)$, as discussed earlier. Theoretically, the M' are expected to increase with temperature. The expression

$$\left(\frac{\partial \ln M'}{\partial \ln \rho}\right)_P = -1$$

is suggested as a first approximation for this effect.

So far we have treated only the variation of the extrinsic or quasi-harmonic effects and showed that they de-

creased with compression. This means that temperature is less effective in causing variations in density and elastic properties in the deep mantle than in the shallow mantle and that relationships between these variations are different from those observed in the laboratory. Anharmonic effects also are predicted to decrease rapidly with compression (Zharkov and Kalinin, 1971; Hardy, 1980; Wolf and Jeanloz, 1985), although experimental confirmation is meager, particularly for the shear constants. Anharmonic contributions are important at high temperature and low pressure, but it is not yet clear whether temperature or pressure dominates in the lower mantle, particularly since the reference temperatures and pressures (such as the Debye, Einstein or melting temperature and the bulk modulus) also increase with compression. Hardy (1980) proposed a convenient measure of anharmonic effects relative to harmonic ones:

$$\lambda = \phi''' \bar{x}/\phi''$$

where ϕ'' and ϕ''', the second and third derivatives of the interionic potential, are the major parameters determining the size of the harmonic and cubic anharmonic effects, respectively, and $\bar{x}$ is the root-mean-square value of the ionic displacements due to thermal motion.

This measure of anharmonicity can be written

$$\lambda = (TR^n)^{1/2}$$

where R is the nearest neighbor distance, T is the absolute temperature and n is the exponent in the power-law repulsive potential, which can be estimated from

$$K_o' = \frac{n + 7}{3}$$

giving $n = 5$ for the lower mantle. The density increases by about 25 percent from zero pressure to the core-mantle boundary. The adiabatic temperature increases by about 33 percent. The increase of A with temperature, therefore, is slightly greater than the decrease associated with compression, suggesting that intrinsic or anharmonic effects remain important in the lower mantle, even if they decrease with pressure. Existing laboratory data neither support nor contradict this supposition.

Model calculations by Raymond Jeanloz (written communication, 1987) suggest that anharmonic contributions are damped more rapidly with compression than quasi-harmonic and harmonic contributions. In fact, the temperature coefficients of the elastic moduli and the anharmonicity decrease exponentially with pressure (Zharkov and Kalinin, 1971). Temperature and pressure have opposing effects, so the relative roles of harmonic (or quasi-harmonic) and anharmonic contributions, particularly for the shear modes, are still uncertain for the high-temperature, high-pressure regime of the lower mantle. Although I have not treated the effect of compression on the anharmonic properties in any detail, the primary conclusions regarding the dominance of rigidity variations in the lower mantle would also follow if pressure suppresses the intrinsic temperature effects on the bulk modulus faster than on the shear modulus. It should be pointed out that the variation of temperature with pressure is different for the Earth than for shock-wave experiments, and therefore the relative role of anharmonicity may be different for these two situations.

The combination of high pressure and low temperature occurs in the vicinity of deep-focus earthquakes in subduction zones. The temperature derivatives of elastic-wave velocities should be particularly low in this situation. The large velocity anomalies associated with slabs may therefore require anisotropy or changes in mineralogy.

ELASTIC PROPERTIES OF COMPOSITE MATERIALS

Rocks are aggregates of several different anisotropic minerals that may differ widely in their properties. They often contain cracks that may be filled with various kinds of fluids. There are various ways to calculate the average properties of heterogeneous materials from the properties of the components. Most of these involve a volume average of randomly oriented components and give the effective isotropic properties.

The classical methods bound the moduli by assuming that the stress or strain is uniform throughout the aggregate:

$$M_R = \left(\sum_{i=1}^{n} v_i/M_i \right)^{-1} \leq \bar{M} \leq \sum_{i=1}^{n} v_i M_i = M_V$$

where M_i is the elastic modulus (K or G) of the i^{th} phase, $\bar{M}$ is the actual modulus of the composite and the subscripts R and V denote the Reuss (uniform stress) and Voigt (uniform strain) averages, respectively; v, is the volume fraction of the i^{th} phase. The effective moduli are often taken as the arithmetic, geometric or harmonic mean of M_i and M_V. If the M_i do not differ widely, then $M_R \approx M_V$ and the method of averaging does not much matter.

For single-phase composites of anisotropic crystals, the effective isotropic moduli are found by averaging over all possible orientations:

$$K_V = \frac{1}{3}(A + 2B)$$

$$G_V = \frac{1}{5}(A - B + 3C)$$

$$A = \frac{1}{3}(C_{11} + C_{22} + C_{33})$$

$$B = \frac{1}{3}(C_{12} + C_{23} + C_{31})$$

$$C = \frac{1}{3}(C_{44} + C_{55} + C_{66})$$

The Voigt moduli depend on only nine of the single crystal moduli even in the most general case of anisotropy where there are 21 independent moduli (see Chapter 15). The Reuss moduli are a similar average over the elastic compliances. Tighter bounds can be placed on the elastic properties of composites by taking into account the interactions between grains and their shapes. The methods can also be generalized to take into account complete or partial orientation of the grains. Hashin and Shtrikman (1963) used a variational principle to bound the properties of composites from above (HS^+) and below (HS^-).

Watt and others (1976) summarized the various averaging techniques and provided a convenient formula for treating several different cases for two-phase aggregates:

$$\frac{\overline{M} - M_1}{M_2 - M_1} = v_2 \left(1 + \frac{v_1(M_2 - M_1)}{M_1 + F} \right)^{-1}$$

where M is K or G, v_1 and v_2 are the volume fractions of the components with moduli M_1 and M_2. The function F is For K:

(HS^+) $$F = 4G_2/3$$

For G:

(HS^+) $$F = G_2(9K_2 + 8G_2)/6(K_2 + 2G_2)$$

for $(G_2 - G_1)(K_2 - K_1) \geq 0$.

For the lower bound (HS-) the subscripts are interchanged. If the inequality is not satisfied, the subscripts of G_1 are interchanged for K and of K_i for G.

LIQUIDS

The liquids that are important in the deep interior of the Earth are silicate magmas and molten iron alloys. Neither of these are simple liquids. Liquids are characterized by fluidity, or low viscosity, and low or vanishing rigidity. An ideal liquid has no order and has zero rigidity. Real liquids have a short-range order and can transmit shear waves of sufficiently high frequency. Most melts are slightly less dense than their crystalline form but are more compressible, so the density difference decreases with pressure. Although liquids generally do not exhibit crystal-like long-range order, they can undergo phase changes that involve coordination changes and the packing of ions. Since solids also undergo such phase changes, the difference between the physical properties of a solid and its melt are not necessarily smoothly varying functions of temperature and pressure. Because of the buffering effect of the latent heat of fusion and the fluidity of melts, it is difficult to raise the temperature of large volumes of the Earth above the temperature of complete melting, the liquidus. Since geophysical fluids are impure, they exhibit a melting interval rather than a distinct melting temperature, and the degree of melting depends on the balance between heat input and heat removal rates and the tendency of the liquid and solid portions of the melt to separate. The largest and most rapid input of energy into the Earth was during original accretion and later large impacts. The rapid ascent of buoyant diapirs can also cause pressure-release melting. The slow process of radioactive heating is unlikely to lead to extensive melting because the processes of conduction and convection efficiently remove the heat.

Even the Earth's outer core is probably close to the melting point and may be a slurry. The inner core is solid, probably an Fe-Ni alloy that is below the melting point because of the high pressure. The outer-core–inner-core boundary, however, is not necessarily the solidus of the material in the core. It may simply represent the boundary at which the liquid fraction of the core is so small that it behaves as a solid to the transmission of seismic waves. A packing of particles with roughly 20 percent fluid-filled voids will behave as a solid. Similarly, the entire outer core may not be above the liquidus. The outer core behaves as a fluid, but it would also do so even if it contained a large fraction of suspended particles. The size of the grains that can be held in suspension depends on their density contrast, the fluid viscosity, the nature of short-range forces and grain interactions and the flow velocity of the core. Solid particles may be continually freezing and refreezing as a parcel of fluid moves around the core. If the outer core is not an ideal fluid, it may have a low but finite rigidity and be anisotropic. Liquid crystals, for example, exhibit such solid-like behavior.

The interatomic potential energy functions for liquids are similar to those for solids. One can usually assume that the total interatomic energy is the sum of the energies of atoms interacting in pairs, the pair potential. The forces between atoms interacting three or more at a time are called many-body forces. Many-body forces are far from negligible in liquid metals. The electrons are not bound to particular atoms but are delocalized over the whole of the material. The "effective pair potentials" for liquid metals are different from those of other liquids.

The interatomic energy is composed of short-range and long-range energies. The long-range energies typically vary at large interatomic distances R as R^{-n}. The Coulombic energy between charges has $n = 1$. Short-range energies are usually assumed to vary as $\exp(-kR)$ at large R. These have their origins in the overlap of orbitals of interacting atoms. The equilibrium interatomic spacing is controlled by the balance between attractive and repulsive potential energies. Elastic properties and their derivatives with pressure depend on derivatives with respect to R of the total interatomic potential energy. The repulsive energy increases rapidly as two atoms are brought close together, so we can consider that atoms and molecules have definite shapes and sizes. For packed hard spheres the repulsive energy rises sharply when R equals the sum of the radii of the

spheres. The "hard sphere" model is quite useful in discussing some of the properties of liquids.

Long-range energies include electrostatic, induction and dispersion energies. The first is calculated from the distribution of charges within the molecules, which is composed of positive charges from the nuclei and a diffuse negative charge from the electrons. The second two depend on how the electrons in the molecule move under the influence of an external electric field, giving a polarization to the molecule.

The simplest pair potential for atoms is the hard-sphere function. For an atom modeled as a hard sphere of diameter d, the potential is zero for R > d and infinite for R < d. This very simple potential, with d determined empirically, is surprisingly useful for those properties that depend primarily on repulsive forces.

Realistic potentials must contain a minimum. The most common form is the power-law potential

$$U(R) = A\left[\left(\frac{r}{R}\right)^{m} - \left(\frac{r}{R}\right)^{n}\right], \quad m > n$$

(where R is ionic radius), which is the Lennard-Jones, or L-J, potential when $m = 12$, $n = 6$. At large R the L-J potential has the correct form for the dispersion energy between closed-shell atoms and molecules. The repulsive part of the potential is steep, as required, but there is no physical significance to m = *12. It* is mathematically convenient to have m = *2n.* An alternative form is

$$U(R) = A\exp(-kR) - CR^{-6}$$

where the constants A and C are found from such data as average interatomic distances and compressibility.

Sound Propagation in Liquid Metals

Metals that have an open-packed crystal structure in the solid state exhibit an increase in coordination upon melting. Most metals, however, experience little change in interatomic distances or coordination when they melt, and some show little change in their physical properties at the melting point. At temperatures slightly above the melting point, metals exhibit a short-range order that becomes more random as the temperature is raised. Electronic and optical properties are well explained by assuming that the conduction electrons are nearly free and interact with the ions through a localized pseudopotential. Other physical properties are explained in terms of a "hole" model of the liquid where the holes (unoccupied electron sites) have a volume, an energy of formation and an activation energy of diffusion. The thermal expansion and compressibility are determined by a certain concentration of holes of definite volume. Properties such as the attenuation of acoustic waves depend on thermal conductivity and shear and volume viscosities. Alloys and eutectics often exhibit complex behavior, including anisotropy and inhomogeneity. At high frequencies or low temperatures, molten metals exhibit some characteristics of crystals, including the ability to transmit shear waves.

Sound velocity generally decreases with rising temperature, and the temperature coefficient is usually much greater than in the equivalent solids, although the variation is sometimes smooth through the melting point. The sound velocity depends on two competing factors, the coordination and the thermal motion of ions.

The sound velocities, for a given valency, decrease with increasing atomic weight. The sound velocity V_p, density ρ, and adiabatic compressibility are related by

$$V_p^2 = (\rho\beta_S)^{-1}$$

The isothermal compressibility is

$$\beta_T = \gamma\beta_S$$

where γ is the Griineisen parameter. Table 6-11 summarizes some properties of liquid metals. The compressibilities of the alkali metals are an order of magnitude larger than those of the noble and polyvalent metals, indicating that the interatomic forces are smaller. The increase of isothermal compressibility through the melting point is generally between *5* and *20* percent.

A metal can be regarded as a lattice of positively charged ions immersed in a sea of conduction electrons. The electron sea about each ion screens its electric field, so that at large distances the Coulomb potential associated with a bare ion of valency z is reduced by an exponential screening factor

$$U(r) \approx (-ze^2/R)\exp(-k_sR)$$

where k_s is a screening parameter. The compressibility is predicted to scale as

$$\beta_S \approx (M/\rho)^{5/3}$$

where M is the atomic weight and Mlp is the atomic volume.

In contrast to a solid, the binding of two atoms in a liquid is a temporary affair. One can view an atom as vibrating with a characteristic period, τ_o, in a temporary equilibrium position and having a characteristic lifetime of τ in this position, where

$$\tau = \tau_o\exp E^*/kT$$

where E* is an activation energy. We can now distinguish several different domains. For rapid processes where $t < \tau$ and $\tau \gg \tau_o$, the fluid has some solid-like characteristics since it does not have time to flow. Thus, high-frequency shear waves can be propagated and short-duration shear stresses can be maintained by an effectively high viscosity. The amplitude of the thermal vibrations of the atoms in a liquid is comparable to the interatomic distance. Therefore, the instantaneous arrangement of the atoms in a liquid possesses a high degree of disorder. However, if we look at the

TABLE 6-11
Elastic Properties and Derivatives of Solid and Liquid Metals

	β_T (Mbar^{-1})		V_p (km/s)		$\left(\frac{\partial \ln V_p}{\partial \ln \rho}\right)_P$	$\left(\frac{\partial \ln V_p}{\partial \ln \rho}\right)_T$
Metal	**Solid**	**Liquid**	**Solid**	**Liquid**	**Liquid**	**Liquid**
Na	16	18.6	3.0	2.6	0.9	1.3
Hg	3	3.8	1.7	1.5	1.7	3.7
In	2.4	3.0	2.6	2.3	1.1	2.2
Sn	1.9	2.7	3.5	2.5	0.9	2.1
Bi	3.0	4.2	2.3	1.6	0	3.3
Zn	1.7	2.5	3.8	2.9	0.7	1.7
Al	1.4	2.4	5.7	4.7	0.8	1.0
Ga	2.0	2.2		2.9	0.8	1.7
Pb	2.6	3.5	2.2	1.8	1.3	2.9
Sb	2.7	4.9	3.4	1.9	−1.1	2.4

Birch (1966), Webber **and Stephens** (1968).

mean positions of particles for $\tau \gg t > \tau_o$, we would see a higher degree of order. The mean positions of the atoms would not change much and a quasi-crystallinity would be displayed, particularly near the melting point. The lifetime of the relative order, however, is small. It increases with pressure and decreases with temperature. For liquid metals it would be of interest to know if convection, electrical currents, magnetic fields and the presence of impurities would allow alignment of these ordered regions giving, for example, a seismic anisotropy. The inner core may be a crystalline solid or have a τ that is longer than the periods of seismic waves, acting therefore as a high-viscosity fluid or a glass.

When a liquid is sampled, or averaged, over periods greater than τ the quasi-crystallinity of the liquid disappears. Translational and other symmetries are not apparent, and the only orderliness is in the average radial distance between atoms, the radial distribution function. Experimental x-ray radial distribution functions refer to this condition rather than the instantaneous or short-time average structure.

Liquid metals exhibit a small excess sound absorption that is attributed to a bulk viscosity caused by an internal arrangement of atoms. The sound wave perturbs these arrangements and energy is thereby extracted by a relaxation process. The amplitude of an acoustic wave of frequency ω propagating in the x direction in a fluid can be written

$$u = u_o \exp - ax \exp i(\omega t - kx)$$

where α is the amplitude absorption coefficient, and k is the wave number. The phase velocity c = wlk. For small attenuation

$$\alpha^* = (2/3)(\eta\omega^2/\rho c^3)$$

where η is the shear viscosity and p is the density. The heating associated with pressure changes in the propagating wave give rise to the flow of heat from the compressed to the dilated parts of the wave. For an ideal gas

$$\alpha^* = \frac{\omega^2 k}{2C_P \rho c^3}(\gamma - 1)$$

where k is the thermal conductivity and C_P is specific heat. Any process that removes energy from the sound wave and returns it at a later time causes dissipation of the acoustic energy. Sound propagation is still adiabatic but is no longer isentropic; that is, there is a production of entropy. The energy removed from the sound wave is transferred to vibration or rotation of atoms or to the potential energy of some structural rearrangement or chemical reaction. The transfer is not instantaneous and is characterized by a relaxation time, τ.

The velocity, $c(\omega)$, varies from the zero-frequency or relaxed value, c_o, to the high-frequency or unrelaxed value, c_∞:

$$c^2/c_o^2 = (1 + \omega^2\tau^2)/[1 + (c_o^2/c_\infty^2)\omega^2\tau^2]$$

The absorption coefficient per unit wavelength A is

$$\lambda\alpha^* = \pi(c^2/c_o^2)\left(\frac{c_\infty^2 - c_o^2}{c_\infty^2}\right)\frac{\omega\tau}{1 + \omega^2\tau^2}$$

The quantity

$$\frac{c_\infty^2 - c_o^2}{c_\infty^2} = 1 - K_S^o/K_S^\infty$$

is the relaxation strength. These equations can be generalized to multiple relaxation mechanisms or a distribution of relaxation times.

The individual relaxation times are

$$\tau = \tau_o \exp E^*/RT$$

where E^* is the activation energy required for an atom to pass from one equilibrium position to another. The height of the potential energy barrier, E^*, is not fixed, as it is in a crystal, but depends on the changing configuration of the atoms in the neighborhood. In the absence of external forces, these barrier jumps are random and no net flow results. If an external force, such as a sound wave, is applied, then flow can result if the period of the wave is greater than T. For short-duration forces, or waves, the flow responds as a solid. Both solid-like and liquid-like behaviors are reflected in the above equations, depending on the frequency of the sound wave or the duration of the applied stress.

The sound (phase) velocity is

$$c^2 = (K_S + 4G/3)/\rho$$

where the rigidity, G, is zero in the low-frequency or relaxed limit. The frequency dependence of the rigidity is

$$G(\omega) = G_\infty \frac{i\omega\tau_s}{1 + i\omega\tau_s}$$

giving a complex sound velocity; that is, an attenuating wave. As $\omega \to \infty$, $G \to G_\infty$. As $\omega \to 0$, $G \to G_o = 0$, and the solid-like property vanishes.

The imaginary part of the shear modulus can be interpreted as a frequency-dependentshear viscosity:

$$\eta(\omega) = \frac{G_\infty \tau_s}{1 + \omega^2\tau_s^2}$$

At low frequencies this reduces to the ordinary shear viscosity

$$\eta = G_\infty \tau_s$$

Similarly, the bulk modulus can be written

$$K = K_o + \frac{K_1\omega^2\tau_c^2}{1 + \omega^2\tau_c^2} + \frac{iK_1\omega\tau_c}{1 + \omega^2\tau_c^2}$$

where K_o is the $\omega = 0$ bulk modulus and $K_o + K_1$ is K_∞, the unrelaxed infinite frequency modulus. If the compressional relaxation time τ_c is similar to the shear relaxation time τ_s, then the attenuation coefficient for longitudinal waves is

$$\alpha^* \simeq (\omega^2/2\rho c^3)(\eta_c + 4\eta_s/3)$$

where η_c is the compressional, or bulk, viscosity.

The effects of pressure and temperature on the absorption coefficient and velocity depend on both the variation of τ and the relaxation strength. Temperature generally decreases τ and c_∞, so the net effect depends on whether $\omega\tau$ is greater than or less than 1. Vibrational relaxation frequencies are expected to increase with pressure because of the smaller interatomic distances and more chances for collisions. Structural relaxation frequencies might be expected to decrease with pressure since it is more difficult for atoms to jump from one state to another.

For simple metals, the temperature and pressure derivatives of the bulk modulus generally satisfy

$$\{K_S\}_P \equiv (\partial \ln K_S/\partial \ln \rho)_P = 2.4 \text{ to } 4.2$$

$$\{K_S\}_T \equiv (\partial \ln K_S/\partial \ln \rho)_T = 3 \text{ to } 7$$

For individual metals

$$(\partial \ln K_S/\partial \ln \rho)_P < (\partial \ln K_S/\partial \ln \rho),$$

which means that there is an intrinsic temperature effect at constant volume. At constant volume the bulk modulus increases with temperature.

The core is invariably treated as an ideal fluid, having zero rigidity at all frequencies. However, real fluids transmit shear waves at high frequency and, therefore, have a finite, if small, rigidity. A viscoelastic fluid can be described as a Maxwell body. The Maxwell time is

$$\tau = \eta/G$$

where η is the shear viscosity and G is the high-frequency rigidity. Such a body will flow without limit under a constant load and therefore behaves as a fluid. At high frequency ($\omega\tau > 1$) the body propagates shear waves with velocity $\sqrt{G/\rho}$. The quality factor, Q, is unity at low frequency and approaches infinity as ω for $\omega\tau > 1$. The quality factor will be discussed in great detail in a later chapter. A Q of unity means high attenuation and of infinity means no attenuation. Low-frequency shear waves have low velocities, approaching zero as $\sqrt{\omega}$, and high attenuation (low Q). Pressure generally increases T, so $\omega\tau$ may increase with depth in the core, giving rise to an effective rigidity for a seismic wave of a given frequency. The rigidity will be lower at free-oscillation periods than at body-wave periods. The periods of normal modes, which are sensitive to properties of the core, may be affected by this rigidity.

The velocity of compressional waves will also be affected by the presence of rigidity and will start to increase with depth when the rigidity starts to have a measurable effect. The bulk modulus of fluids is also affected by relaxation effects operating through the bulk viscosity.

Properties of Oxide Melts

The volumes and bulk moduli of silicate melts can be approximated by averaging the properties of the component oxides. The bulk moduli are approximately

$$K = (K_V + K_R)/2$$

where

$$K_V = \Sigma V_i K_i$$

$$K_R = (\Sigma(V_i/K_i))^{-1}$$

and V_i are the volume fractions of components i.

The molar volumes of oxide melts are usually about 10–20 percent more than the crystalline components. The

TABLE 6-12
Molar Volumes V_0, Thermal Expansivities α and Bulk Moduli K_0 for Components in Silicate Liquids at 1400°C and Solids at 25°C

	Melts			Crystals		
Oxide	V_0 ($cm^3/gf\omega$)	α ($\times 10^5$/K)	K_0 (kbar)	V_0 ($cm^3/gf\omega$)	α ($\times 10^5$/K)	K_0 (kbar)
SiO_2	27.08	1.0	130	22.69	3.5	378
Al_2O_3	36.83	6.2	209	25.56	1.6	2544
FeO	13.31	23.6	745* 287†	12.12	3.5	1740
MgO	11.87	23.4	888* 386†	11.28	3.1	1630
CaO	16.49	24.3	49.4	16.76	3.8	1140
Na_2O	28.82	24.7	135	—	—	—
K_2O	46.05	26.1	82	—	—	—

Rivers and Carmichael (1986), Herzberg (1987)
*From fusion curve.
†From ultrasonics.

bulk moduli of the melts are considerably less than the solids. The low bulk moduli mean that the volumes of melts and crystals converge at high pressure. Table 6-12 gives the properties of components of oxide melts and solids. Details are given in the Herzberg reference.

General References

Anderson, D. L. (1988) Temperature and pressure derivatives, J. *Geophys. Res.*, *93*, 4688–4700.

Anderson, O. L., E. Schreiber, R. C. Liebermann and N. Soga (1968) Some elastic constant data on minerals relevant to geophysics, *Rev. Geophys.*, 6, 491–524.

Bina, C. and B. Wood (1987) J. *Geophys. Res.*, *92*, 4853.

Bonzcar, L. J., E. K. Graham and H. Wang (1977) The pressure and temperature dependence of the elastic constants of pyrope garnet, J. *Geophys. Res.*, *82*, 2529–2534.

Chang, Z. P. and G. R. Barsch (1973) Pressure dependence of single-crystal elastic constants and anharmonic properties of spinel, J. *Geophys. Res.*, *78*, 2418–2433.

Chang, Z. P. and G. R. Barsch (1969) Pressure dependence of the elastic constants of single-crystalline magnesium oxide, J. *Geophys. Res.*, *74*, 3291–3294.

Chang, Z. P. and E. K. Graham (1977) Elastic properties of oxides in the NaCl-structure, J. *Phys. Chem. Solids*, *38*, 1355–1362.

Frisillo, A. L. and G. R. Barsch (1972) Measurement of single-crystal elastic constants of bronzite as a function of pressure and temperature, J. *Geophys. Res.*, *75*, 6360–6384.

Graham, E. K. and G. R. Barsch (1969) Elastic constants of single-crystal forsterite as a function of temperature and pressure, J. *Geophys. Res.*, *74*, 5949–5960.

Jones, L. E. A. (1979) Pressure and temperature dependence of the single crystal elastic moduli of the cubic perovskite $KMgF_3$, *Phys. Chem. Mineral.*, *4*, 23–42.

Jones, L. E. A. and R. C. Liebermann (1974) Elastic and thermal properties of fluoride and oxide analogues in the rocksalt, fluorite, rutile and perovskite structures, *Phys. Earth Planet. Inter.*, 9, 101–107.

Kumazawa, M. and 0 . L. Anderson (1969) Elastic moduli, pressure derivatives, and temperature derivatives of single-crystal olivine and single-crystal forsterite, J. *Geophys. Res.*, *74*, 5961–5972.

Liu, H. P., R. N. Schock, and D. L. Anderson (1975) Temperature dependence of single-crystal spinel ($MgAl_2O_4$) elastic constants from 293 to 423°K measured by light-sound scattering in the Raman-Nath region, *Geophys. J. R. Astr. Soc.*, *42*, 217–250.

Manghnani, M. H. (1969) Elastic constants of single-crystal rutile under pressures to 7.5 kilobars, J. *Geophys. Res.*, *74*, 4317–4328.

Simmons, G. and H. Wang (1971) ***Single-Crystal Elastic Constants and Calculated Aggregate Properties: A Handbook,*** 2nd ed., The M.I.T. Press, Cambridge, MA.

Skinner, B. J., Thermal expansion, in S. P. Clark (ed.) (1966) Handbook of Physical Constants, *Geol. Soc. Am., Mem. 97, Sect. 6*, 78–96.

Soga, N. (1967) Elastic constants of garnet under pressure and temperature, J. *Geophys. Res.*, *72*, 4227–4234.

Spetzler, H. (1970) Equation of state of polycrystalline and single-crystal MgO to 8 kilobars and 800°K, J. *Geophys. Res.*, *75*, 2073–2087.

Surnino, Y. (1979) The elastic constants of Mn_2SiO_4, Fe_2SiO_4 and Co_2SiO_4 and the elastic properties of olivine group minerals at high temperature, J. *Phys. Earth.*, *27*, 209–238.

Sumino, Y., O. L. Anderson and I. Suzuki (1983) Temperature coefficients of elastic constants of single crystal MgO between 80 and 1,300 K, *Phys. Chem. Minerals,* 9, 38–47.

Sumino, Y., O. Nishizawa, T. Goto, I. Ohno and M. Ozima (1977) Temperature variation of elastic constants of single-crystal forsterite between −190 and 400°C, *J. Phys. Earth., 25,* 377–392

Watt, J. P., G. F. Davies and R. J. O'Connell (1976) The elastic properties of composite materials, *Rev. Geophys. Space Phys., 14,* 541–563.

Weidner, D. V. (1986) in Chemistry and Physics of Terrestrial Planets, ed. S. K. Saxena, Springer-Verlag, New York, 405 pp.

Weidner, D. J., J. D. Bass, A. E. Ringwood and W. Sinclair (1982) The single-crystal elastic moduli of stishovite, *J. Geophys. Res., 87,* 4740–4746.

Weidner, D. J. and N. Hamaya (1983) Elastic properties of the olivine and spinel polymorphs of Mg_2GeO_4, and evaluation of elastic analogues, *Phys. Earth Planet. Inter., 33,* 275–283.

Weidner, D. J. and E. Ito (1985) Elasticity of $MgSiO_3$ in the ilmenite phase, *Phys. Earth Planet. Int., 40,* 65–70.

Weidner, D. J., H. Sawamoto, S. Sasaki, and M. Kumazawa (1984) Single-crystal elastic properties of the spinel phase of Mg_2SiO_4, *J. Geophys. Res., 89,* 7852–7860.

References

Ahrens, T. J., D. L. Anderson and A. E. Ringwood (1969) Equations of state and crystal structures of high-pressure phases of shocked silicates and oxides, *Rev. Geophys., 7,* 667–702.

Anderson, D. L. (1987) A seismic equation of state, II. Shear and thermodynamic properties of the lower mantle, *Phys. Earth Planet. Inter., 45,* 307–323.

Anderson, O. L. (1986) Simple solid state equations for materials of terrestrial planet interiors, Proceedings NATO Conference on Physics of Planetary Interiors.

Basset al. (1981) *Phys. Earth Planet. Int., 25,* 140, 181.

Bassett, W., T. Takahashi, H. Mao and J. Weaver (1968) Pressure .induced phase transition in NaCl, *J. Appl. Phys., 39,* 319–325.

Birch, F. (1961) The velocity of compressional waves in rocks to 10 kilobars, Part 2, *J. Geophys. Res., 66,* 2199–2224.

Birch, F. (1966) *Handbook of Physical Constants,* S. P. Clark, Jr. (ed.), *Geol. Soc. Am.,* Memoir 97.

Birch, F. (1968) Thermal expansion at high pressures, *J. Geophys. Res., 73,* 817–819.

Boehler, R. (1982) Adiabats of quartz, coesite, olivine and MgO at 50 kbar and 1000 K, and the adiabatic gradient in the Earth's mantle, *J. Geophys. Res., 87,* 5501–5506.

Brillouin, L. (1964) *Tensors in Mechanics and Elasticity,* Academic Press, New York.

Butler, R. and D. L. Anderson (1978) Equation of state fits to the lower mantle and outer core, *Phys. Earth Planet. Inter., 17,* 147–162.

Clayton, R. W. and R. P. Comer (1983) A tomographic analysis of mantle heterogeneities from body wave travel times, *Eos, 62,* 776.

Davies, G. (1976) *Geophys. J. Astron. Soc., 44,* 625–648.

Doyle, H. A. and A. L. Hales (1967) An analysis of the travel times of S waves to North American stations, *Bull. Seis. Soc. Am., 57,* 761–771.

Dziewonski, A. M. (1984) Mapping the lower mantle: Determination of lateral heterogeneity in P velocity up to degree and order 6, *J. Geophys. Res., 89,* 5929–5952.

Dziewonski, A. M. and D. L. Anderson (1981) Preliminary reference Earth model, *Phys. Earth Planet. Inter.,* 25, 297–356.

Hager, B. H., R. W. Clayton, M. A. Richards, R. P. Comer, and A. M. Dziewonski (1985) Lower-mantle heterogeneity, dynamic topography, and the geoid, *Nature, 313,* 541–545.

Hardy, R. J. (1980) Temperature and pressure dependence of intrinsic anharmonic and quantum corrections to the equation of state, *J. Geophys. Res., 85,* 7011–7015.

Hashin, Z. and S. Shtrickman (1963) *J. Mech. Phys. Solids, 11,* 127–140.

Herzberg, C. J. (1987) *Magmatic Processes: Physiochernical Processes,* the Geochemical Society, Special Publication.

Jeanloz, R. and T. J. Ahrens (1980) *Geophys. J. R. Astro. Soc., 62,* 505–528.

Jeanloz, R. and E. Knittle (1986) Reduction of mantle and core properties to a standard state by adiabatic decompression. In *Chemistry and Physics of Terrestrial Planets* (S. K. Saxena, ed.), 275–305, Springer-Verlag, Berlin.

Jones, L. (1976) *Phys. Earth Planet. Interiors, 13,* 105–118.

Jones, L. (1979) Pressure and temperature dependence of the single crystal elastic moduli of the cubic perovskite $KMgF_3$, *Phys. Chem. Min., 4,* 23–42.

Knittle, E., R. Jeanloz and G. L. Smith (1986) Thermal expansion of silicate perovskite and stratification of the Earth's mantle, *Nature, 319,* 214–216.

Knittle, E. R. and R. Jeanloz (1987) *Science, 235,* 668–670.

Knopoff, L. (1963) Solids: Equations of state at moderately high pressures. In *High Pressure Physics and Chemistry (R.* S. Bradley, ed.), 227–245, Academic Press, New York.

Nakanishi, I. and D. L. Anderson (1982) World-wide distribution of group velocity of mantle Rayleigh waves as determined by spherical harmonic inversion, *Bull. Seis. Soc. Am., 72,* 1185–1194.

Nataf, H.-C., I. Nakanishi and D. L. Anderson (1984) Anisotropy and shear-velocity heterogeneities in the upper mantle, *Geophys. Res. Lett., 11,* 109–112.

Nataf, H.-C., I. Nakanishi and D. L. Anderson (1986) Measurements of mantle wave velocities and inversion for lateral heterogeneities and anisotropy, Part III, Inversion, *J. Geophys. Res., 91,* 7261–7307.

Richards, M. A. (1986) Dynamical models for the Earth's geoid, Ph.D. Thesis, California Institute of Technology, Pasadena, 273 pp.

Rivers, M. and I. Carmichael (1986) *J. Geophys. Res.* (in press).

Sumino, Y. and O. L. Anderson (1984) Elastic constants of miner-

als. In ***Handbook of Physical Properties of Rocks,*** v. ***III*** (R. S. Carmichael, ed.), 39–138, CRC Press, Boca Raton, Florida.

Suzuki, I., O. L. Anderson and Y. Sumino, Elastic properties of a single-crystal forsterite Mg_2SiO_4, up to 1,200K, ***Phys. Chem. Minerals, 10,*** 38–46, 1983.

Svendsen and Ahrens (1983) ***Geophys. Res. Lett., 10,*** 501–540.

Wallace, ***D.*** C. (1972) ***Thermodynamics of Crystals,*** Wiley, New York.

Watt, J. P., G. F. Davies and R. J. O'Connell (1976) The elastic properties of composite materials, ***Rev. Geophys. Space Phys.,*** 14, 541–563.

Webber, G. M. B. and R. W. B. Stephens (1968) ***Physical Acoustics IVG,*** W. ***P.*** Mason (ed.), Academic Press, N.Y.

Wolf and Bukowinski (1986) ***High Pressure Research in Geophysics,*** eds. M. Manghnani and Y. Symo.

Wolf, G. and R. Jeanloz (1985) Vibrational properties of model monatomic crystals under pressure, ***Phys. Rev.*** B, ***12,*** 7798–7810.

Woodhouse, J. H. and A. M. Dziewonski (1984) Mapping the upper mantle: Three-dimensional modeling of earth structure by inversion of seismic waveforms, ***J. Geophys. Res., 89,*** 5983–5986.

Yagi, Ida, Sato and Akimoto (1975) ***Phys. Earth Planet. Int., 10,*** 348–354.

Yamamoto, S. and O. L. Anderson (1986) Elasticity and anharmonicity of potassium chloride at high temperature, ***J. Phys. Chem. Minerals*** (in press).

Yamamoto, S., I. Ohno and 0 . L. Anderson (1986) High temperature elasticity of sodium chloride, J. ***Phys. Chem. Solids*** (in press).

Zharkov, V. and V. Kalinin (1971) *Equations* ***of State for Solids at High Pressures and Temperatures,*** Consultants Bureau, New York, 257 pp.